JIPB Journal of Integrative Plant Biology

Research Article
https://doi.org/10.1111/jipb.13078

Phylotranscriptomic insights into Asteraceae diversity, polyploidy, and morphological innovation[oo]

Caifei Zhang[1†], Chien-Hsun Huang[1,2†], Mian Liu[1], Yi Hu[2], Jose L. Panero[3], Federico Luebert[4,5], Tiangang Gao[6] and Hong Ma[2*]

1. State Key Laboratory of Genetic Engineering and Collaborative Innovation Center of Genetics and Development, Ministry of Education Key Laboratory of Biodiversity Sciences and Ecological Engineering, Institute of Biodiversity Sciences, Institute of Plant Biology, Center for Evolutionary Biology, School of Life Sciences, Fudan University, Shanghai 200438, China
2. Department of Biology, the Huck Institutes of the Life Sciences, the Pennsylvania State University, University Park, Pennslyvania 16802, USA
3. Department of Integrative Biology, The University of Texas, University Station C0930, AustinTexas 78712, USA
4. Institut für Bodiversität der Pflanzen, Universität Bonn, Bonn D – 53115, Germany
5. Department of Silviculture and Nature Conservation, University of Chile, Santiago 9206, Chile
6. State Key Laboratory of Evolutionary and Systematic Botany, Institute of Botany, the Chinese Academy of Sciences, Beijing 100093, China
†These authors contributed equally to this work.
*Correspondence: Hong Ma (hxm16@psu.edu)

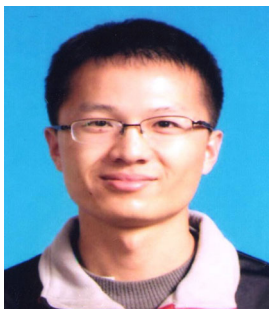

Caifei Zhang

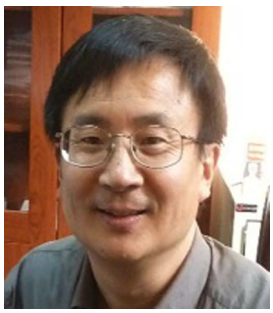

Hong Ma

ABSTRACT

Biodiversity is not evenly distributed among related groups, raising questions about the factors contributing to such disparities. The sunflower family (Asteraceae, >26,000 species) is among the largest and most diverse plant families, but its species diversity is concentrated in a few subfamilies, providing an opportunity to study the factors affecting biodiversity. Phylotranscriptomic analyses here of 244 transcriptomes and genomes produced a phylogeny with strong support for the monophyly of Asteraceae and the monophyly of most subfamilies and tribes. This phylogeny provides a reference for detecting changes in diversification rates and possible factors affecting Asteraceae diversity, which include global climate shifts, whole-genome duplications (WGDs), and morphological evolution. The origin of Asteraceae was estimated at ~83 Mya, with most subfamilies having diverged before the Cretaceous–Paleocene boundary. Phylotranscriptomic analyses supported the existence of 41 WGDs in Asteraceae. Changes to herbaceousness and capitulescence with multiple flower-like capitula, often with distinct florets and scaly pappus/receptacular bracts, are associated with multiple upshifts in diversification rate. WGDs might have contributed to the survival of early Asteraceae by providing new genetic materials to support morphological transitions. The resulting competitive advantage for adapting to different niches would have increased biodiversity in Asteraceae.

Keywords: biodiversity, compositae, morphological character evolution, phylogeny, transcriptome, whole-genome duplication

Zhang, C., Huang, C.H., Liu, M., Hu, Y., Panero Jose, L., Luebert, F., Gao, T., and Ma, H. (2021). Phylotranscriptomic insights into Asteraceae diversity, polyploidy, and morphological innovation. J. Integr. Plant Biol. **63:** 1273–1293.

INTRODUCTION

Biodiversity, by its simplest definition, is the number of species within a given boundary, and is a crucial indication of ecosystem health (Loreau et al., 2001), with increasing significance for human society. Biodiversity varies dramatically among different groups of related extant organisms, including between sister lineages (Harmon, 2012;

Rabosky et al., 2012). In land plants, the angiosperms (flowering plants, ~369,000 species) and gymnosperms (~1 050 species) are two sister lineages with strikingly different species numbers (Lughadha et al., 2016). Asteraceae are one of the two largest angiosperm families, comprising ~26,000 species or about 7% of extant flowering plants (Funk et al., 2009a; Christenhusz and Byng, 2016; Panero and Crozier, 2016; Wills, 2017). Asteraceae include several crops (e.g., sunflower, lettuce, artichoke), medicinal herbs, and ornamental plants, and share several floral characteristics, including a compact inflorescence (the capitulum or head) comprising one to >1,000 flowers surrounded by one or more series of involucral bracts (Leins and Erbar, 2010). The Asteraceae species richness is much greater than related families in the order Asterales, including Calyceraceae (47 spp.), Campanulaceae (2,340 spp.), Goodeniaceae (430 spp.), and Menyanthaceae (60 spp.). Asteraceae subfamilies also vary greatly in species numbers, from one species (Famatinanthoideae and Hecastocleidoideae) to approximately 17,200 species (Asteroideae). Among the other subfamilies, the next three largest are Cichorioideae (3,994 spp.), Carduoideae (2,864 spp.), and Mutisioideae (637 spp.), with the others each containing fewer than 100 species (Panero and Crozier, 2016). Asteraceae is therefore an excellent family for the analysis of the variation in biodiversity between related groups, including the possible impacts of past climate changes and morphological innovations.

Morphological and molecular evolutionary analyses require a well-resolved phylogeny. Previous analyses, largely using plastid genes, have supported the monophyly of Asteraceae (Anderberg et al., 2007), defining 45 tribes in 13 subfamilies (Funk et al., 2014; Panero et al., 2014). The relationships among the Asteraceae subfamilies and most tribes have also been resolved using plastid sequences (Fu et al., 2016; Panero and Crozier, 2016), although some uncertainties remain. In recent years, nuclear genes have been successfully used to resolve relationships among deep angiosperm lineages and within orders and families (Zeng et al., 2014, 2017; Yang et al., 2015; Xiang et al., 2016; Huang et al., 2016a; Zhang et al., 2020); for example, the relationships in Asteraceae have been analyzed using 175 or fewer nuclear genes from ~70 or fewer species (representing up to eight of the 13 subfamilies) (Mandel et al., 2017; Liu et al., 2015; Huang et al., 2016b). More recently, Mandel et al. (2019) used specific probes to capture up to 935 nuclear loci from 256 species (representing all 13 subfamilies) using largely Hyb-Seq of genomic DNAs to reconstruct the Asteraceae phylogeny in supermatrix and coalescent (ASTRAL) approaches. These results differed from the previous plastid sequence-based phylogenies in terms of the monophyly of, and relationships among, some subfamilies, with additional differences at the tribal level among the trees generated using different methods. Moreover, while the supermatrix trees supported the monophyly of Asteraceae, the coalescent tree placed a species of Calyceraceae, a previously well-supported sister family of Asteraceae, as nested within Asteraceae with low support (Mandel et al., 2019) (Figure S1). Thus, it is important to further examine Asteraceae phylogenetic relationships in additional analyses.

Whole genome duplications (WGDs) are widespread in the angiosperms and are implicated in evolutionary innovations and species diversifications (Jiao et al., 2011; Cannon et al., 2015; Li et al., 2015; Soltis et al., 2015; Yang et al., 2015; Barker et al., 2016; Xiang et al., 2016; Huang et al., 2016b). Various numbers (one to 17) of WGDs have been proposed to have occurred in Asteraceae, including one for the core Asteraceae consistently supported by genomic, phylogenomic, and Ks analyses of some or all of Asteroideae, Cichorioideae, Carduoideae, and Mutisioideae (Barker et al., 2008, 2016; Huang et al., 2016b; Badouin et al., 2017; Reyes-Chin-Wo et al., 2017; Leebens-Mack et al., 2019; Zhang et al., 2020). Another WGD event was detected for the clade encompassing the multi-tribe group called the "Heliantheae alliance" (containing Heliantheae, Eupatorieae, and other tribes) (Smith, 1975; Robinson, 1981; Yahara et al., 1989; Berry et al., 1995; Gentzbittel et al., 1995; Baldwin et al., 2002), which was also supported by analyses using Ks distribution (Barker et al., 2008) and phylogenomic methods (Huang et al., 2016b; Leebens-Mack et al., 2019). However, these previous molecular studies sampled fewer than 70 species of Asteraceae; thus, a further examination of the dates and associated taxon lineages of Asteraceae WGDs using a greater number of taxa is needed to gain insights into their possible contribution to Asteraceae biodiversity.

Here, we report the identification of 1,087 nuclear genes from the transcriptomes and genomes of 243 Asteraceae species (including 29 species overlapping with those sampled by Mandel et al. (2019)) representing all 13 subfamilies, and the reconstruction of highly supported and well-resolved Asteraceae phylogenies using both supermatrix and coalescent approaches with these nuclear genes. Our analyses allowed a comprehensive comparison of our Asteraceae phylogenies with those reported by Mandel et al. (2019). Furthermore, we present results on the divergence times of the Asteraceae lineages, shifts of diversification rates, phylotranscriptomic evidence for 41 WGDs, and the reconstruction of ancestral morphological characters. Moreover, we discuss the possible contributions of environmental changes, WGDs, and morphological innovations to the high biodiversity of Asteraceae.

RESULTS AND DISCUSSION

Asteraceae nuclear phylogeny reveals highly supported relationships among subfamilies

To reconstruct a tribal-level Asteraceae phylogeny, 243 Asteraceae species were sampled, representing all 13 subfamilies and 41 of the 45 recognized tribes (Panero and Funk, 2008; Funk et al., 2009b; Panero et al., 2014; Fu et al., 2016; Huang et al., 2016b) (149 species in Asteroideae, e.g., sunflowers, daisies, and chrysanthemums; 27 in Cichorioideae, e.g., lettuce and dandelion; 33 in

Carduoideae, e.g., artichoke and thistles; and five outgroup taxa). We newly generated transcriptome and genome sequences from 121 (for one species, RNAs from two samples were sequenced) and 16 species, respectively (see Supporting Information; Tables S1, S2), plus 67 previous datasets from our lab (Zeng et al., 2014; Liu et al., 2015; Huang et al., 2016b) and 44 publicly available datasets (Tables S1, S2). To reduce possible biases caused by the use of a particular approach, we used three separate approaches to identify low-copy nuclear genes for the phylogenetic analyses (see Figure S2A for a flow chart on gene selection and Supporting Information for details).

Phylogenetic analyses using both coalescent and maximum likelihood (ML) methods with multiple datasets comprising nuclear genes yielded highly supported and consistent Asteraceae phylogenies (Figures 1, 2, S3, S14) (see Supporting Information for details). Asteraceae were monophyletic in all analyses here, forming a sister clade to Calyceraceae (three genera sampled), and the phylogeny was mostly consistent with previously reported topologies (e.g., Panero and Funk, 2008; Panero et al., 2014; Fu et al., 2016; Panero and Crozier, 2016). Asteroideae and seven other subfamilies were monophyletic with 100% support in all analyses; Famatinanthoideae and Hecastocleidoideae were monotypic; whereas Wunderlichioideae, Cichorioideae, and Carduoideae were not monophyletic (Figure 1). Seven relatively small subfamilies formed a grade of six successive sister branches of all the other Asteraceae: (i) Barnadesioideae (~92 spp.); (ii) Famatinanthoideae (one sp.); (iii) a clade with the subfamilies Mutisioideae (~640 spp.) and Stifftioideae (35 spp.), and the tribe Hylideae (13 spp.) of Wunderlichioideae, with the topology (Mutisioideae (Stifftioideae, Hylideae)); (iv) the tribe Wunderlichieae (34 spp.) of Wunderlichioideae (supported by 100% bootstrap support (BS) values in four trees and 98% BS in the fifth tree; Figure S15); (v) Gochnatioideae (85 spp.); and (vi) Hecastocleidoideae (one sp.).

Mandel et al. (2019) reported that Barnadesioideae were sister to the other Asteraceae species in the supermatrix trees only, whereas their relationships with Calyceraceae and the remaining Asteraceae were poorly resolved in the coalescent tree (Figure S1). Furthermore, the phylogenetic relationships of Famatinanthoideae, Mutisioideae, Stifftioideae, and Hylideae in the two supermatrix trees presented by Mandel et al. (2019) were the same as in our phylogeny; however, in their coalescent tree, Famatinanthoideae were sister to a clade comprising Stifftioideae and Hylideae (97% BS), with Mutisioideae being the next sister group separating them from the remaining Asteraceae (71% BS). Moreover, Wunderlichieae, Gochnatioideae, and *Cyclolepis* (not sampled here) formed a clade (64% BS/1.0 Bayesian posterior probability (PP) in the supermatrix trees; and 100% BS in the coalescent tree), although the placement of *Cyclolepis* was inconsistent (Figure S1). Further studies are therefore needed to clarify the phylogenetic positions of Wunderlichieae, Gochnatieae, and *Cyclolepis*.

Several clades, including Hylideae, Mutisioideae, and Stifftieae, were highly supported in all our analyses as well as in the supermatrix analyses presented by Mandel et al. (2019). Previously, Hylideae were found to be sister to Wunderlichieae and were thus placed in Wunderlichioideae (*s.l.*) (52/71/84% BS; 0.91/0.998/0.99 PP) in analyses performed using 10–14 plastid loci (Panero and Funk, 2008; Panero et al., 2014; Panero and Crozier, 2016). By contrast, analyses using nuclear ITS sequences (91% BS/1.0 PP; Funk et al. (2014)) and numerous protein-coding nuclear genes (here and also by Mandel et al. (2019)) all highly supported the sister relationship of Hylideae and Stifftieae.

Among the remaining Asteraceae, Pertyoideae (~80 spp.) are sister to an extremely large clade (>24,000 spp.) that includes the three largest subfamilies, Asteroideae, Cichorioideae, and Carduoideae, as well as two very small subfamilies, Corymbioideae and Gymnarrhenoideae (Figures 1, 2). This position of Pertyoideae is also supported by recent analyses using ITS data (Funk et al., 2014) and hundreds of nuclear sequences (Funk et al., 2014; Mandel et al., 2019) (Figure S1). However, in plastid-based phylogenies, Pertyoideae are sister to the clade Gymnarrhenoideae–Asteroideae (Panero and Funk, 2008; Panero et al., 2014; Panero and Crozier, 2016). Pertyoideae are the only subfamily in which distribution is restricted to East Asia, and that produce corollas with five irregularly split lobes intermediate between the typical ligulate (such as those of Cichorieae) and tubular flowers (such as those in Cardueae and some Asteroideae). In addition, the basal chromosome numbers in Pertyoideae are $x = 12–15$ (Wang, 2009; Zhang, 2013), unlike the presumed ancestral Asteraceae chromosome number of nine (Semple and Watanabe, 2009). Nevertheless, some morphological features of Pertyoideae, such as short style branches with papillae on the abaxial surface and relatively simple pollen surfaces, resemble those of the early-divergent branches of the Asteraceae rather than Carduoideae (Katinas et al., 2008). Among the single-gene family trees of the 192 genes in set 11 (Figure S2), the position of Pertyoideae reported here was supported by 52 trees with BS values of more than 75%, and by 97 additional trees with BS values between 50% and 75%, but no trees supported the previously published placement based on the analyses of plastid genes (e.g., Panero and Funk, 2008; Panero et al., 2014; Fu et al., 2016; Panero and Crozier, 2016). Future studies with expanded sampling could improve our understanding of the placement of Pertyoideae.

The mostly Old World subfamilies Carduoideae and Cichorioideae, as previously defined (Funk et al., 2014; Panero et al., 2014; Fu et al., 2016), were paraphyletic in all of our phylogenetic analyses. All four tribes in Carduoideae formed two clades, which are indicated, respectively, as Carduoideae I and II (Figure S15, and abbreviated, respectively, as Ca-I and Ca-II in Figures 1, S1). Carduoideae I includes three

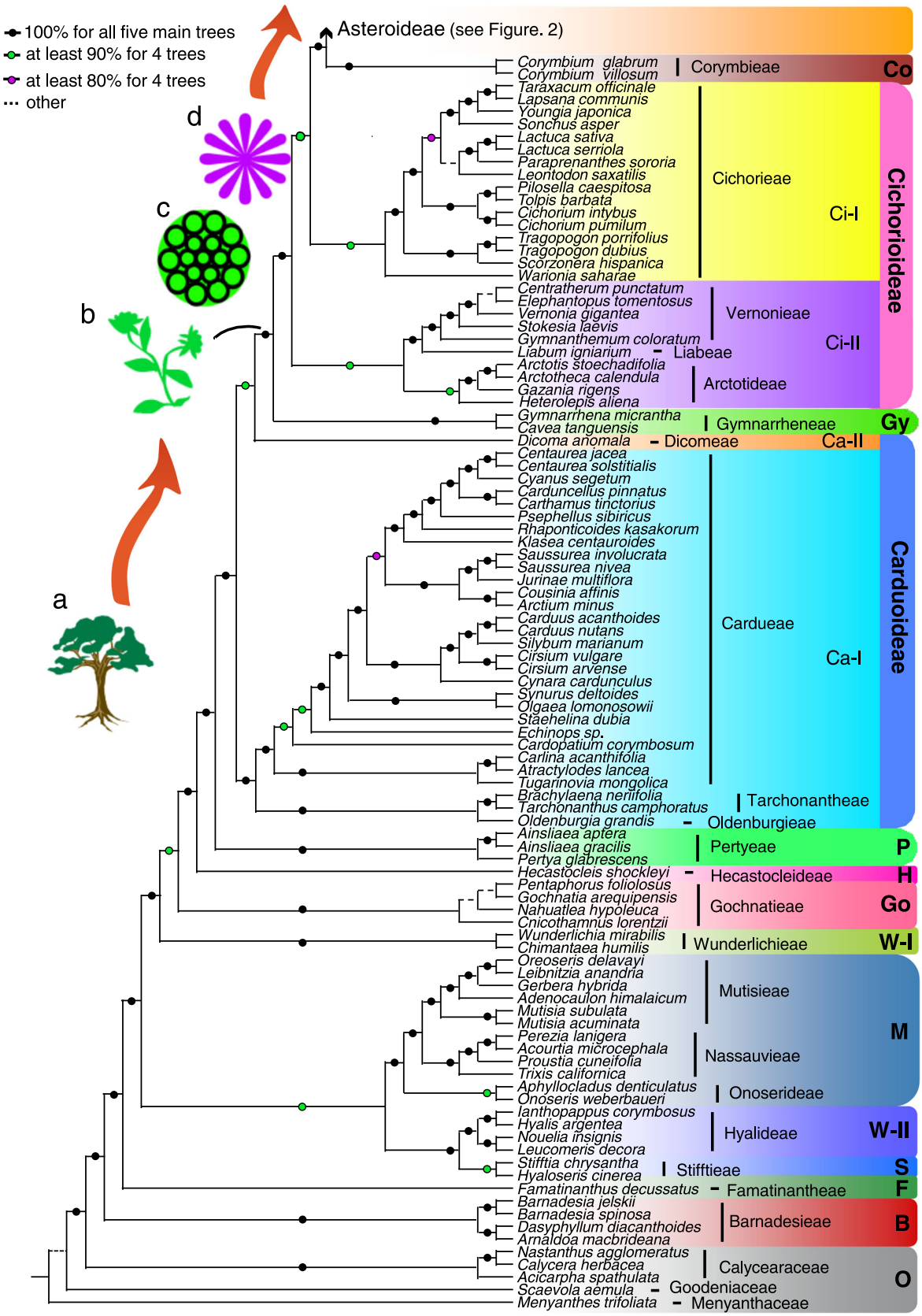

Figure 1. Continued

tribes, Cardueae, Oldenburgieae, and Tarchonantheae, with maximum support, whereas Carduoideae II contains the fourth small tribe, Dicomeae, which is consistently placed as sister (BS values of 100%, 90%, 89%, 87%, and 87%; Figure S15) to the clade Gymnarrhenoideae–Asteroideae. Carduoideae I (Figures 1, S1, S15) is the sister lineage to the clade Carduoideae II–Asteroideae. The coalescent (ASTRAL) tree presented by Mandel et al. (2019) grouped all four tribes of Carduoideae in a single clade, whereas the supermatrix ML analyses placed the combined Tarchonantheae and Oldenburgieae clade, the Dicomeae clade, and the Cardueae clade as three separate branches in a grade of successive sisters to the clade of Gymnarrhenoideae–Asteroideae (Figure S1). On the other hand, phylogenies using plastid genes strongly supported the inclusion of Dicomeae in the Carduoideae (Fu et al., 2016; Panero and Crozier, 2016). Gene flow among Dicomeae, Cardueae, Tarchonantheae, and Oldenburgieae and the underlying assumptions of the different methods used are possible explanations for the different relationships seen in these phylogenies.

The circumscription of Cichorioideae has changed several times, even very broadly, from containing only one tribe, Cichorieae, to encompassing all Asteraceae members other than Asteroideae (see review by Funk and Chan, 2009). The recent definition of the Cichorioideae was based on analyses using plastid sequences (Funk et al., 2014; Panero et al., 2014; Fu et al., 2016), but it lacks the support of morphological synapomorphy. Among the four Cichorioideae tribes sampled here, Cichorieae (Figures 1, S1, S15) were sister to the clade Asteroideae + Corymbioideae (BS = 89–100% in the four phylogenies) (Figure S15). On the other hand, three other tribes, Vernonieae, Liabeae, and Arctotideae, form a clade (BS of 100%, 100%, 99%, and 93%) sister to the clade Asteroideae + Corymbioideae + Cichorieae (Figure 1). The paraphyly of Cichorioideae was also supported by Mandel et al. (2019) (Figure S1). Thus, Cichorieae are proposed as Cichorioideae *s.s.* (indicated as Cichorioideae I in Figure S15, and abbreviated as Ci-I in Figures 1, S1), whereas the other three tribes, Vernonieae, Liabeae, and Arctotideae, are proposed to form a separate subfamily (indicated as Cichorioideae II in Figure S15 and abbreviated as Ci-II in Figures 1, S1). The difference in the position of Cichorieae relative to the other tribes between the phylogenies using nuclear or chloroplast genes could be explained by a possible hybridization in the history of Cichorieae.

Resolution of the relationships among the Asteraceae tribes

In addition to the relationships among Asteraceae subfamilies, the nuclear phylogenies here also provide strong support for the relationships among tribes (Figures 1, 2, S3–S15). Among the 41 tribes in this study, 30 were monophyletic with 100% support (Figures 1, 2), but in the subfamily Asteroideae, Millerieae and Neurolaeneae were not monophyletic (Figure 2). The remaining nine tribes were represented by one species each (two corresponding to monotypic subfamilies). In addition to the relationships among subfamilies of Asteraceae, the nuclear phylogenies generated here also provide strong support for the relationships among tribes (Figures 1, 2, S3–S15). The vast majority of the tribes represented in this study were also sampled in Mandel et al. (2019) (Figure S1), except Polymnieae (*Polymnia*) in Asteroideae (Figures 2, S1). The sister relationship of Mutisieae and Nassauvieae, and that of Oldenburgieae and Tarchonantheae, were both also supported by phylogenies developed using plastid genes (Panero and Funk, 2008; Panero et al., 2014) and nuclear genes (Mandel et al., 2019). Within Cichorioideae II, the tribes Vernonieae and Liabeae are sisters, but more distant to Arctotideae (Figure 1), consistent with their positions in previous phylogenetic analyses (Figure S1). In Arctotideae, *Heterolepis* (Arctotideae III) is sister to Arctotideae I (Arctotidinae) in our analyses, but sister to Arctotideae II (Gorteriinae) in the analyses performed by Mandel et al. (2019) (Figure S1), and it has varying positions in previous analyses performed using different datasets and different outgroups (Funk et al., 2004, 2009a). Future analyses with other methods and more taxon sampling may shed light on the relationships among *Heterolepis* and other Arctotideae species.

The subfamily Asteroideae were previously divided into three supertribes: Asterodae, containing four tribes; Helianthodae, containing 15 tribes; and Senecionodae, with only one tribe, Senecioneae (Robinson, 2004). The analyses performed here (Figures 2, S15) support the monophyly of

Figure 1. A portion of the Asteraceae phylogeny showing all subfamilies, except Asteroideae, and summaries of character reconstruction

The phylogeny is shown for all subfamilies except Asteroideae, using coalescence analyses using four gene sets (set 4: 1,087 genes; set 5: 649 genes; set 7: 384 genes; set 11: 192 genes) and maximum likelihood (ML) analysis using 192 genes (set 11) obtained as explained in Figure S2 (see Supporting Information for details). The individual phylogenies are shown in Figures S3–S14, with support values shown in Figure S15. To the right of generic/specific names are tribe names, with subfamily names abbreviated as follows: B, Barnadesioideae; F, Famatinanthoideae; S, Stifftioideae; W-II, Wunderlichioideae-II; M, Mutisioideae; W-I, Wunderlichioideae-I; Go, Gochnatioideae; H, Hecastocleidoideae; P, Pertyoideae; Gy, Gymnarrhenoideae; Co, Corymbioideae. The subfamilies Cichorioideae and Carduoideae are paraphyletic and are indicated with two vertical bars, with the clades labeled as Ci-I/Ci-II and Ca-I/Ca-II, respectively. The change of habit from woody (a) to herbaceous (b) according to ancestral character reconstruction (Figure S36) is estimated to have occurred at the root node of Gymnnarrhenoideae – Asteroidaee. The change of capitulum type is according to the analysis shown in Figure S39 and shown here from an ancestral and basal discoid with only disc florets (c) to ligulate capitulum with only ligulate florets (d) in the subfamily Cichorioideae and radiate capitulum (e in Figure 2) characterized by having both ray and disc florets and found in most members of Asteroideae and some in Cichorioideae II.

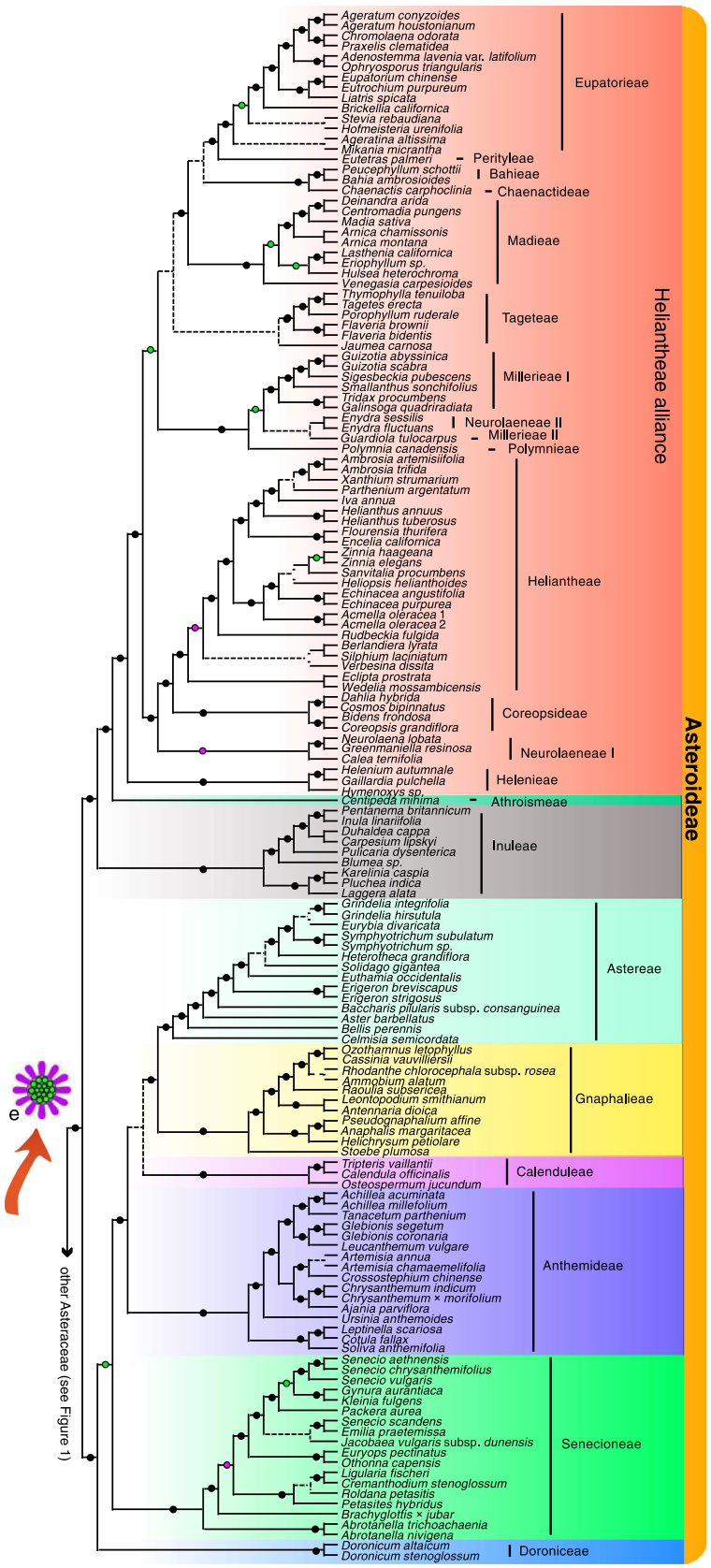

Figure 2. Continued

Asterodae with 100% BS. Among the four Asterodae tribes, Astereae and Gnaphalieae were sister clades (100% BS), with Anthemideae and Calenduleae splitting successively and as sister to the other Asterodae. Although the sister relationship between Astereae and Gnaphalieae was also recovered in nuclear phylogenies performed by Liu et al. (2015) using 49 nuclear genes and by Mandel et al. (2019), Anthemideae were placed differently in previous analyses, either as sister to Astereae with high support in plastid phylogenies (Panero and Funk, 2008; Panero et al., 2014; Panero and Crozier, 2016), or as sister to Senecioneae in nuclear phylogenies with limited samplings by Liu et al. (2015) and from the supermatrix analyses with 75% BS in Mandel et al. (2019) (Figure S1). The previously reported sister relationship between Anthemideae and Senecioneae suggested that Asterodae might not be monophyletic. This, in combination with Astereae and Anthemideae being sisters in the plastid phylogenies, led Liu et al. (2015) to propose a hybrid origin of Anthemideae from a cross between parental lineages related to Astereae and Senecioneae, respectively, which was also supported by some morphological characters (see discussion by Liu et al., 2015). By contrast, the sister relationship of Anthemideae and Senecioneae was supported by nuclear gene analyses of three species in each tribe (Liu et al., 2015), and in 12 and 16 species in Anthemideae and Senecioneae, respectively (Mandel et al., 2019). However, this reported phylogenetic relationship did not include the Senecioneae genus *Abrotanella*, which have disciform capitula with four-lobed corollas, unlike most Senecioneae, which have discoid or radiate capitula with five- and/or three-lobed corollas (Nordenstam, 2007). The sampling here included 16 Anthemideae species in 12 genera and 18 Senecioneae species in 14 genera, including two *Abrotanella* species. Our findings placed *Abrotanella* as sister to the other Senecioneae with maximal support (Figure 2). The maximally supported monophyly of Asterodae (including Anthemideae) and Senecioneae (including *Abrotanella*) suggested that the increased sampling or inclusion of *Abrotanella* here was important for achieving the highly supported resolution of these groups, and does not support Senecioneae as a possible parental lineage of Anthemideae.

In addition, the genus *Doronicum* was resolved here as sister to the combined clade of Asterodae and other members of Senecioneae (Figures 2, S15), supporting its designation as the tribe Doroniceae proposed by Panero (2005) and adopted by Fu et al. (2016) in their systematic arrangements for Asteraceae from China. *Doronicum* was not sampled by Mandel et al. (2019). *Doronicum* was traditionally placed in Senecioneae, primarily according to gross morphology; however, its relationship with members of the Senecioneae was poorly resolved in the ITS- and plastid-based phylogenies (Pelser et al., 2010; Fu et al., 2016). Consequently, *Doronicum* was not assigned to a previously defined Senecioneae subtribe (Nordenstam et al., 2009). The strongly supported position of *Doronicum* here clearly separates it from Senecioneae and argues for its designation as a distinct tribe. Both *Doronicum* and *Abrotanella* were members of Senecionodae (Nordenstam, 2007), but the phylogeny generated here suggests that Senecionodae are not monophyletic.

The supertribe Helianthodae contains 15 tribes, all sampled here except for the monotypic Feddeeae (Figure 2). The relationships we identified among the Helianthodae tribes are consistent with those reported by Mandel et al. (2019), except for some taxa that were only sampled here, including one tribe (Polymnieae, containing *Polymnia*) and three genera (*Enydra*, *Guardiola*, and *Jaumea*, in the tribes Neurolaeneae, Millerieae, and Tageteae, respectively). All phylogenies herein provide strong support for the monophyly of the supertribe and seven of the 10 tribes containing two or more species: Bahieae, Coreopsideae, Eupatorieae, Helenieae, Heliantheae, Inuleae, and Madieae. In contrast, Tageteae were monophyletic only in the ML analysis of 192 genes (set 11); *Jaumea* did not group with other Tageteae genera in the coalescent phylogenies (Figures S3–S15), similar to results of the analysis using plastid sequences (Fu et al., 2016). Moreover, Millerieae and Neurolaeneae were not monophyletic; the genus *Enydra* (two species sampled here; previously in Neurolaeneae (Panero, 2007)) was nested within the Millerieae, which were represented here by six genera. In a previous plastid phylogeny (Fu et al., 2016), *Enydra* was sister to a clade of three other Neurolaeneae genera (also sampled here), but the grouping of *Enydra* with the other Neurolaeneae was not strongly supported (<50% BS/0.95 PP). Millerieae and *Enydra* are both pantropical, whereas the other Neurolaeneae are all restricted to the Americas (Panero, 2007). Thus, the phylogenetic position of *Enydra* among Millerieae genera and their geographical distribution may support a proposed expansion of Millerieae to include *Enydra*.

Among the Helianthodae tribes, Inuleae and Athroismeae were successively diverged from the other tribes with maximum support, and the remaining tribes formed a strongly supported clade, referred to as the "Heliantheae alliance" (Panero, 2007; Baldwin, 2009) (Figures 2, S15). Within the Heliantheae alliance, Helenieae were the first to diverge, with

Figure 2. A portion of the Asteraceae phylogeny with subfamily Asteroideae and summaries of character reconstruction
The phylogeny shown here is for the largest subfamily Asteroideae, with 20 of its 21 tribes (except Feddeeae), summarized from results as described in the legend of Figure 1. The morphological change from discoid (c in Figure 1) to radiate (e) with both ray and disc florets, according to the ancestral character reconstruction is detailed in Figure S39. The latter type is found in most members of Asteroideae, with an important exception being members of the tribe Eupatorieae, which likely lost the ray florets following the separation from the small tribe Perityleae.

the other tribes forming three major clades. The first major clade includes Neurolaeneae (excluding *Enydra*), Heliantheae, and Coreopsideae. Members of these groups produce head inflorescences with bracts (referred to as paleae or receptacular bracts) subtending the florets/achenes. Heliantheae and Coreopsideae were strongly supported sisters (Figure 2), which was also supported by previous analyses using ITS data (Baldwin et al., 2002) or dozens of nuclear genes (Liu et al., 2015); however, different topologies were recovered using plastid sequences (Jansen et al., 1991; Panero and Funk, 2002; Panero et al., 2014). The inconsistent positions of Coreopsideae between the nuclear and plastid phylogenies were potentially due to hybridization events (Panero, 2007; Liu et al., 2015), which might also be true for Heliantheae. In the second clade we identified with six tribes, Eupatorieae and Perityleae were strongly supported as sisters (Figure 2), as were Bahieae and Chaenactideae, in agreement with previous studies (Panero and Funk, 2002; Panero and Crozier, 2016). Tageteae were sister to Madieae and the weakly supported clade ((Chaenactideae, Bahieae), (Perityleae, Eupatorieae)). These six tribes are mostly epaleate (Panero, 2007).

The third major clade was sister to the second clade and contains Millerieae + *Enydra* + Polymnieae, the latter of which contains only one genus, *Polymnia*, with three species distributed in eastern North America. The Neurolaeneae genus *Enydra* is pantropical, whereas Millerieae genus *Guardiola* is mostly found in Mexico and is aquatic (Figure 2). *Polymnia* is superficially similar to other genera in Millerieae but was placed in the Heliantheae subtribe Polymniinae by Robinson (1978), who considered most species previously placed in *Polymnia* to be members of the genus *Smallanthus* (Millerieae). Polymnieae were once placed in Millerieae as the subtribe Polymniinae (Robinson, 1978), but in the plastid phylogenies they constituted a distinct clade separate from other Millerieae species (Panero and Funk, 2002; Panero, 2007). Moreover, most members of Millerieae were closely related to Heliantheae in the plastid phylogenies, but *Enydra* was included in the Neurolaeneae clade (Panero, 2007; Panero and Funk, 2008); these differences in nuclear and plastid phylogenies thus suggest a possible hybrid origin.

Asteraceae origin was estimated in the Late Cretaceous, while most tribes diverged before the Oligocene

Environmental factors play major roles in shaping biodiversity. To obtain clues about possible historical environmental influences on biodiversity in Asteraceae, we estimated the times of the origins of, and divergences among, the Asteraceae lineages using the newly reconstructed nuclear phylogeny (Figures 1, 2) and the 192 nuclear genes (set 11 in Figure S2). We performed molecular clock analyses using calibrations with 15 fossil constraints, including seven Asteraceae fossils (Table S2), and a secondary calibration for the crown node of the Eudicots (Zanne et al., 2014; Tank et al., 2015). A fossil pollen, *Tubulifloridites lilliei* type A (referred as *Tl*-typeA hereafter) was reported as being related to early members of Asteraceae, but with uncertain placement (Barreda et al., 2015). To test the effects of the use and position of *Tl*-typeA on age estimation, it was either not included (calibration set 1) or included with differing placements (sets 2–5) (see Supporting Information for details). The results from the r8s and BEAST analyses were nearly identical among calibration set 1 and sets 3–5 (Figures S16–S25); thus, only the results from using calibration sets 1 and 2 are discussed below.

The mean ages were similar along the backbone from the r8s and BEAST analyses using the same calibration set (Figure 3; Table S3). Particularly, the estimated ages of the most recent common ancestors (MRCAs) of Asteraceae, Calyceraceae, Goodeniaceae to Menyanthaceae, and of Heliantheae alliance varied by no more than 3 My between the two methods. Variations of 10–15 My were found in the ages of some lineages, such as Cichorioideae I, Carduoideae I, and Cichorioideae II. On the other hand, estimations with the fossil calibration set 1 (without the pollen fossil) and set 2 (with the pollen fossil at the position assigned by Barreda et al., 2015) performed using the same method differed by fewer than 10 My for most nodes, except those of the crown Barnadesioideae and one of its two subclades (the MRCA of *Dasyphyllum* and *Arnaldoa*) (Figures S26, S27). Thus, the results from both methods and each fossil calibration set all suggest the origin of Asteraceae in the middle of the Late Cretaceous, with the separation of the subfamilies before or near the Cretaceous–Paleocene boundary at ~66 Mya, and divergence of most of the tribes before the Oligocene, or during the Eocene or Paleocene (Figure 3). Gymnarrheneae, Cardueae, Pertyeae, Hecastocleideae, Gochnatieae, Wunderlichieae, Famatinantheae, and Barnadesieae probably arose before the end of the Cretaceous (Figure 3).

Including *Tl*-typeA on the *Dasyphyllum* stem led to an estimated age of the crown Asteraceae similar to those reported by Barreda et al. (2015); however, this result (set 2) differed substantially from those with different placements of *Tl*-typeA (sets 3–5). The estimated ages of the crown Asteraceae from the latter three placements were similar to each other and to the age estimated without the inclusion of *Tl*-typeA, indicating an obvious impact of assigning *Tl*-typeA to *Dasyphyllum*. Because this placement is controversial (Panero, 2016), we accept the more conservative and consistent results from the other four estimations and discuss the ages from calibration set 1 below. Using calibration set 1, Asteraceae and its sister clade, Calyceraceae, were estimated to have diverged ~83 Mya. The Barnadesioideae then separated from the other Asteraceae subfamilies ~81 Mya, with seven other subfamilies progressively diverging during the next 10 My. Throughout the late Cretaceous when these subfamilies separated, the climate was much warmer and more humid than the present (Linnert et al., 2014), suggesting that higher temperatures might have promoted early Asteraceae diversification (Davies et al., 2004; Jablonski et al., 2006; Jansson and Davies, 2008).

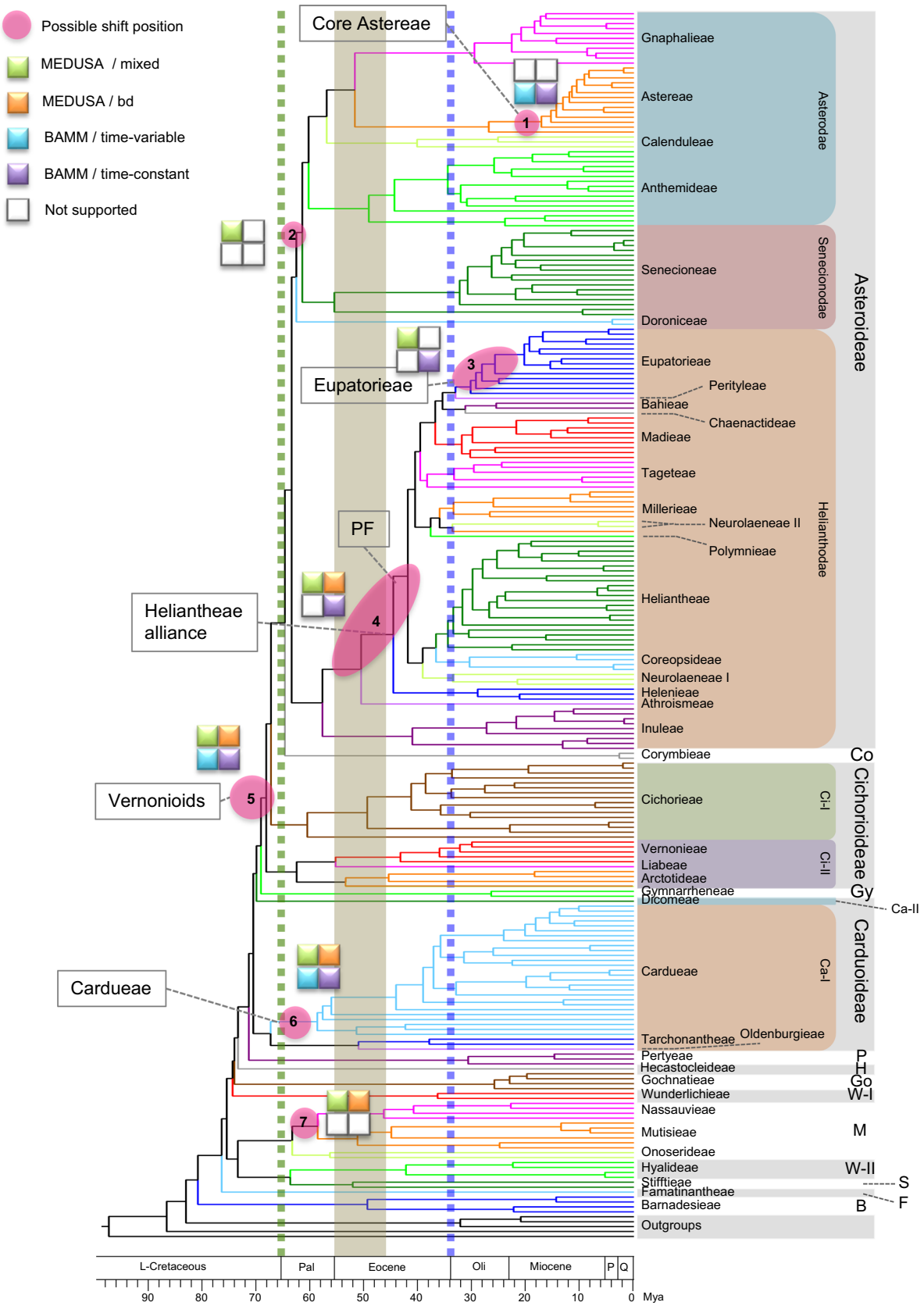

Figure 3. Continued

Except for Stifftioideae, all other subfamilies, including the three largest subfamilies (Asteroideae, Cichorioideae, and Carduoideae, comprising 69%, 16%, and 11% of Asteraceae species, respectively) (Panero and Crozier, 2016), diverged before the Cretaceous–Paleocene boundary when massive extinctions occurred (at 66 Mya) (Figure 3) (Jablonski and Chaloner, 1994). Also, the supertribes Asterodae and Helianthodae and the tribe Senecioneae (Figure 3) separated ~62–61 Mya, with further divergences of most of the ~20 Asteroideae tribes in the Eocene. Further divergences among some tribes/subtribes, and also genera, occurred after the Eocene–Oligocene boundary alongside great climate changes and numerous extinctions (Ivany et al., 2000). In addition to the possible roles of climate factors, the massive extinctions at the Cretaceous–Paleocene and Eocene–Oligocene boundaries, which likely freed numerous ecological niches, could therefore also have facilitated the diversification of the largest subfamily, Asteroideae.

The ages estimated here are generally older than those reported in previous studies, including the estimated age of the Asteraceae stem of ~50 My reported in studies with sampling at higher (e.g., across several families or orders) or lower (e.g., of a tribe) taxonomic levels (Bremer et al., 2004; Barres et al., 2013; Beaulieu et al., 2013; Jabaily et al., 2014; Magallón et al., 2015; Park and Potter, 2015; Tank et al., 2015). The ages estimated here using calibration set 1 (Figures 3, S16, S17) are also older than those reported by Panero and Crozier (2016) using 11 plastid genes and one noncoding region (85 species in 39 tribes), such as the age estimated here for the crown Asteraceae of ~81 My compared with the ~65 My reported by Panero and Crozier (2016). However, our estimated age for the crown Asteraceae is close to that (83 Mya) reported by Mandel et al. (2019). The differences in estimated ages might be due to the sequence datasets (nuclear vs. plastid genes), gene numbers, and/or taxon sampling, as well as the calibrations (Table S2).

Multiple increases in the diversification rate in the Asteraceae

Changes in species richness could be due to either increases or decreases in diversity, which could be estimated by the analysis of shifts in the rate of diversification using a reference phylogeny. To better understand the history of diversity changes in Asteraceae, we estimated the diversification rates and identified the approximate positions of rate shifts during Asteraceae evolution using the MEDUSA (Alfaro et al., 2009) and BAMM methods (Rabosky, 2014; Rabosky et al., 2014b; Shi and Rabosky, 2015). The positions with potential major accelerations in net diversification rate obtained using both methods (each with two different models) are collectively illustrated in Figure 3. For the analyses using MEDUSA (with mixed and birth–death models; Figures S28, S29), we collapsed the tree tips to the tribal level and used the species number of each tribe as the species richness. The result showed six accelerations in net diversification rates (red circles) and one deceleration (blue circle) (Figure S28). Among the upshifts, four with 2.7-, four-, three-, and twofold increases relative to the background (circles 2–5), respectively, are associated with the Vernonioid clade (Asteroideae–Cichorioideae II), the Heliantheae alliance excluding Heleneae (also called the phytomelanic (dark-colored) fruit (PF) clade), the tribe Eupatorieae, and the clade comprising two supertribes (Asterodae and Senecionodae). Rate accelerations were also found at nodes leading to the Nassauvieae + Mutisieae clade and the tribe Cardueae, resulting in approximately twofold increases in the diversification rate.

We also used BAMM with the complete tree in Figure 3 and the sampling fraction data (Table S4), performing separate analyses using both time-variable and time-constant algorithms. Both algorithms produced the same best shift configurations (the one with maximum a posteriori probability; MAP configuration) with three rate shifts (Figure S30): at the Vernonioid clade (circle 5), the Cardueae clade (circle 6), and the core Astereae clade (circle 1). These shifts can also be observed in the rate through time plots (Figure S30). The shifts at the Helianthodae alliance/PF (circle 4) and the Eupatorieae clade (circle 3) were also supported by BAMM under the time-constant algorithm in a further investigation of the results (Figures S32–S34; Table S10).

In summary, all four analyses performed here strongly support upshifts of the net diversification rates at the Vernonioid clade (circle 5) and at tribe Cardueae (circle 6) (Figure 3), affecting the largest subfamilies, Asteroideae, Cichorioideae II (Vernonioideae), and Carduoideae. The next likely position for a diversification rate upshift is among the nodes from the PF clade to the Heliantheae alliance, and may even include Athroismeae (circle 4); finding an event here possibly benefited from a greater sampling of this tribe. This group is positioned within the large supertribe Helianthodae and includes many tribes that further expanded after the Eocene–Oligocene boundary during the dramatic climate changes and mass extinctions. Another possible upshift took place near the divergence of Eupatorieae (circle 3), which expanded greatly after the Eocene–Oligocene boundary. Mutisieae (or the Mutisieae + Nassauvieae clade) (circle 7) is

Figure 3. Molecular clock estimates of divergence times and diversification rate shifts in Asteraceae

This figure presents the subtree containing members of Asterales retrieved from the result of age estimation with calibration set 1. Green and blue dotted lines indicate the boundaries of Cretaceous-Paleocene and Eocene-Oligocene, respectively. The brown stripe corresponds to the hottest period of the Cenozoic era. Multiple specific molecular clock analyses are shown in Figures S16–S27. The positions for increases of net diversification rate resulting from individual analyses are collectively depicted with colored circles. Colored blocks indicate the analysis supporting a shift at the indicated position. Detailed results from each analysis are shown in Figures S28–S34.

another group with a possible rate increase that expanded after the Cretaceous–Paleocene boundary. Similarly, the clade Asterodae + Senecioneae and the core Astereae also had possible diversification rate increases; the earlier divergence among the tribes occurred after the Cretaceous–Paleocene boundary, whereas the later divergence within Astereae took place after the Eocene–Oligocene boundary. Among these, the upshifts at the PF and Vernonioid clades (circles 4 and 5) were also reported by Panero and Crozier (2016), and those marked with circles 2 and 4 were consistent with those proposed by Mandel et al. (2019).

Detection of multiple WGD events

Several WGDs have previously been detected in Asteraceae using genomic, phylogenomic, and Ks analyses of 70 or fewer species (Barker et al., 2008, 2016; Huang et al., 2016b; Badouin et al., 2017; Reyes-Chin-Wo et al., 2017; Leebens-Mack et al., 2019; Zhang et al., 2020). The newly resolved Asteraceae phylogeny generated here from large-scale datasets of 243 species representing all subfamilies and almost every tribe provide an unprecedented opportunity to detect Asteraceae WGDs and place them phylogenetically. We investigated WGD by reconstructing trees of 5 282 orthologous groups (OGs) and comparing them with the reference phylogeny, detecting numerous clusters of gene duplications (GDs) as evidence for a WGD at one of multiple nodes of the Asteraceae phylogeny (see Materials and Methods). According to the strength of the GD evidence, we propose nine WGDs and 32 candidate WGDs (Figures 4, S35), including WGD1 shared by Calyceraceae and Asteraceae, WGD2 shared by the core Asteraceae (Asteroideae–Mutisioideae/Stifftioideae), and WGD3/WGD4 at successive nodes shared by tribes of the Heliantheae alliance (without/with Helenieae, respectively).

WGD1 and WGD2 have also been detected in previous studies (Barker et al., 2016; Huang et al., 2016b), and are consistent with those reported in analyses including multiple angiosperm families and small numbers of Asteraceae species (the XASTβ event described by Leebens-Mack et al., 2019), and WGD #23 described by Zhang et al. (2020)). It is worth noting that, following WGD2, the chromosome base number decreased from 27 to 10, and the species dispersed from South America to Africa/Asia–Eurasia (Funk and Chan, 2009; Semple and Watanabe, 2009). After WGD3, the chromosome base number changed once again from 10 to 19, and the species dispersed from Africa/Asia–Eurasia to North America (Funk and Chan, 2009; Semple and Watanabe, 2009). However, in our analysis, WGD3 shows much fewer GDs than WGD4 (301 vs. 782, respectively), and most of the GDs are of the Type II pattern (~87%), indicating that only one gene copy was detected in Helenieae species in most OGs (Figure 4C, 4D). WGD4 (without Helenieae) is also consistent with the XASTα event described by Leebens-Mack et al. (2019). These results have three possible explanations: (i) the WGD event occurred at the Heliantheae alliance (WGD3), but both copies were lost in Helenieae for most OGs; (ii) the WGD event occurred at WGD3, but the variable substitution rates among the Helenieae and other lineages of the Heliantheae alliance caused many of the gene duplications to apparently support WGD4; or (iii) there was a hybridization event between Helenieae and the ancestor of the other Heliantheae alliance species shortly after their divergence.

There are also large numbers of GDs at the crown node of the subfamilies Gochnatioideae (WGD5) and Pertyoideae (WGD6); and within the tribes Mutisieae (WGD7), Senecioneae (WGD8), Anthemideae (WGD9), and Gnaphalieae (WGD10) (Figure 4B). We also detected 31 other clusters of GDs, providing evidence for candidate WGDs (Supporting Information text; Figure S35). In summary, previous studies using a relatively small number of species (Barker et al., 2016; Huang et al., 2016b; Leebens-Mack et al., 2019) and the present analysis with much greater sampling reached the same conclusion about WGDs at nodes shared by many lineages (WGD1, WGD2, and WGD3/WGD4). In addition, other tribes have experienced independent WGD events, affecting groups with very high species richness (>1 000 species). Of the 32 candidate WGDs (Figure S35), a large majority were detected in the largest subfamilies, including 19 events in Asteroideae, three in Cichorioideae (including the tribe Cichorieae), and two in Carduoideae. Nevertheless, some WGDs were associated with small subfamilies or tribes, such as Gochnatioideae (~70 spp.), Pertyoideae (~80 spp.), and Mutisieae (~254 spp.), suggesting that a WGD alone might not be sufficient for increased diversity and that other factors, such as environmental conditions, are also important. This is consistent with a previous analysis of multiple WGDs throughout the angiosperms (Ren et al., 2018).

Ancestral states of morphological characters

Morphological innovations can afford evolutionary advantages and promote divergence and biodiversity; therefore, we examined the morphological evolution of Asteraceae in the context of the nuclear phylogeny presented here with the aim of identifying a link between morphological innovation and organismal diversity. We traced the ancestral states and histories of seven evolutionarily significant characters, including the habit, pappus, and five floral traits (Figures S36–S42). The Asteraceae ancestor was most likely woody, with epaleate receptacles, a solitary homogamous capitula with isomorphic and discoid florets, and a capillary/plumose pappus, which is largely consistent with the estimations of Bremer (1994) and Panero et al. (2014). One important morphological change along the backbone is from the ancestral woody habit to the herbaceous habit (Figures 1, S36) at the last common ancestor of multiple subfamilies, including the Gymnarrhenoideae and Asteroideae, with a likelihood value 0.948. This estimated change in habit is older than the root node of the Cichorioideae–Asteroideae (0.899) estimated by Panero et al. (2014). It is possible that the transition to herbaceousness could have occurred later than the estimate here, as our sampling did not include some of the woody

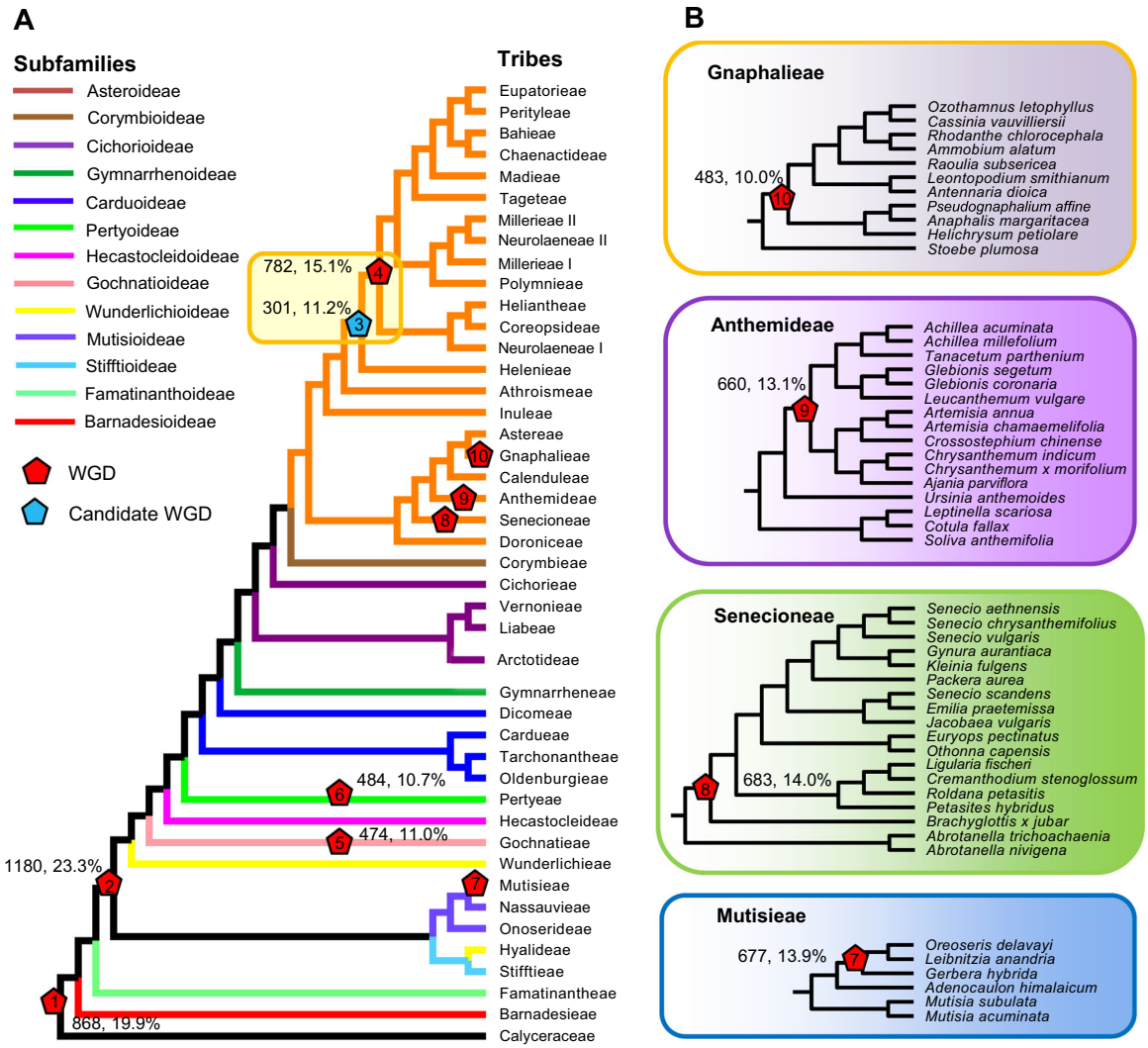

Figure 4. Continued

species in Cichorioideae II (Karis et al., 2009; Robinson, 2009; Robinson and Funk, 2009). Regardless of the precise position of the transition to the herbaceous habit, the woody habit in early Asteraceae history is supported by the woodiness of members of the subfamilies Barnadesioideae, Famatinanthoideae, Stifftioideae, Wunderlichioideae, Gochnatioideae, Hecastocleidoideae, and Pertyoideae in a grade of early divergent sister lineages of most of Asteraceae. This is further supported by the presence of woody members in the tribes Onoserideae and Nassauvieae, as successive sisters of other Mutisioideae, and in the tribes Oldenburgieae and Tarchonantheae that form a sister clade to the Cardueae (Figure S36). On the other hand, most members of the large subfamilies Asteroideae and Cichorioideae (*s.l.*) and the tribe Cardueae are herbaceous, although habit transitions have also occurred later in Asteraceae history, even among closely related species (e.g., Panero et al., 1999), with woody members in these groups likely derived secondarily from herbs.

Asteraceae are characterized by a head inflorescence (capitulum) with sessile florets surrounded by bract-like organs in a compact structure (Funk et al., 2009b), which can be solitary or part of a higher order inflorescence (capitulescence) (Figure S37). The florets in a capitulum can be uniformly bisexual (homogamous) or exhibit sexual differentiation between the outermost and inner florets (heterogamous) (Figure S38). In addition, the corolla of florets exhibits several morphologies, including the actinomorphic (radially symmetric) disc florets found in several subfamilies, the zygomorphic (bilaterally symmetric) ligulate florets of Cichorieae, and the zygomorphic ray florets on the periphery of heads exemplified by members of Asteroideae. Thus, discoid heads contain only disc florets, radiant heads have marginal disc florets with an enlarged corolla, while ligulate heads contain only ligulate florets, which have a corolla with a five-lobed outer lip. Radiate capitula are found in sunflowers (*Helianthus*) and most Asteroideae, and comprise outer pistillate or neutral ray florets and inner bisexual disc florets. On the other hand, in disciform heads, the outer florets are pistillate but lack the large corolla of ray florets.

The ancestral character analysis here supports an inflorescence transition from solitary to capitulescence prior to the divergence of the clade Hecastocleidoideae (0.983) (Figure S37), similar to the estimation of Panero et al. (2014). The homogamous and discoid capitulum were estimated as the ancestral state at the Asteraceae root node (with 99.36% and 99.95% likelihood values, respectively) (Figures S38, S39). Previously the ancestral discoid capitulum had a likelihood value of only 48% (Panero et al., 2014), probably because of differences in the coding of capitulum type for some taxa in Mutisioideae and Hyalideae. In these groups, the outer florets have zygomorphic corollas with a tri-lobed outer lip and a much smaller bi-lobed inner lip. Thus, these capitula are referred to as radiate-like and are different from the true radiate capitula, which have no inner lip in the corolla of outer florets. The genes contributing to the formation of radiate-like capitula and radiate capitula are also different (Chen et al., 2018). In most Asteroideae, heterogamous and radiate capitula are the symplesiomorphies; the morphological and sexual differentiations between outer ray florets and inner disc ones make the capitulum function as a single larger flower. These large "flower-like" heads are again often arranged in a group or series. Such higher order inflorescences (capitulescences) have been recognized as having great success in attracting pollinators (Stuessy et al., 1986; Celep et al., 2014), thereby contributing to the diversification of this largest Asteraceae subfamily comprising more than 15 000 species. Radiate capitula were also found to have arisen independently in Arctotideae, Liabeae, and Oldenburgieae. On the other hand, the transition of radiate to discoid or disciform capitula, the outer florets of which lack the large outer lip of rays, was estimated to have occurred independently several times, with one affecting the entire Eupatorieae tribe.

In most Asteraceae, the floret calyx persists after anthesis and is called the pappus. The pappus remains attached to the inferior fruit (achene) during fruit development and even after maturity. It has different morphological types, such as capillary (hair-like), plumose (feather-like), and scaly. Some Asteraceae also have a bract-like organ (called the palea, or receptacular bract) subtending all or some florets on a receptacle. Both the pappus and the palea serve to protect the developing fruit, and the pappus often facilitates the dispersal of achenes, such as by wind for dandelion and many others (Stuessy and Spooner, 1988; Stuessy and Garver, 1996). Some Asteraceae members lack the pappus (and are therefore epappose); these taxa are found mostly in the Anthemideae and partly in the Heliantheae alliance, and generally possess receptacular bracts (Stuessy and Garver, 1996). In the present study, the pappus was estimated to be capillary (64.7%) or plumose (30.0%) for the root node of Asteraceae. More specifically, the capillary pappus was supported to be the ancestral state for most nodes except the earliest divergent clade containing Barnadesioideae and the Heliantheae alliance. This is different from the Asteraceae ancestral state of a scaly pappus with a defensive function

Figure 4. A summary of whole-genome duplications (WGDs) detected in Asteraceae

(**A**) The lineages in each of 13 subfamilies are represented by colored lines. Nine detected WGDs are marked as red pentagons, with one candidate WGD (WGD3) marked as a blue pentagon, with the detected GD numbers and percentages. (**B**) The node of WGDs within four tribes are marked. (**C**) Three types of the topologies of retained duplicates are illustrated. For the two sub-clades of taxa derived from one node, Type I has retention of both duplicates in both subclades. Type II lacks one copy in the small sub-clade (blue), and Type III lacks one copy in the large sub-clade (red). (**D**) The ratio of three types of the nine WGDs and the candidate WGD (WGD3). Additional information for WGD events is shown in Figure S35.

proposed by Stuessy and Garver (1996). The most common pappus type in Barnadesioideae is the plumose pappus (Stuessy et al., 2009), which likely facilitates seed dispersal over a greater distance. Considering the origin and early evolution of Asteraceae in much warmer climates and more closed habitats (e.g., forest) than the conditions today, the dispersal function of a plumose/capillary pappus would be more important in the early evolution of Asteraceae. On the other hand, the defense function of a scaly pappus would be more important against herbivores, especially for many species of the Heliantheae alliance with larger achenes. For the Heliantheae alliance, various kinds of scaly pappus and paleate receptacles for the protection and dispersal of achenes might have contributed to the successes and increase in diversity of this large and diverse group containing 11 tribes.

In short, Asteraceae have experienced several morphological changes, including the transition from a woody to herbaceous habit, from homogamous capitula with isomorphic florets to heterogamous capitula with differentiated florets, from a discoid capitulum to other types with zygomorphic florets in several large subfamilies, including radiate-like (Mutisioideae), ligulate (Cichorioideae I), and radiate (most Asteroideae and tribes in Cichorioideae II/Vernonioideae). The formation of paleate receptacles and variously modified pappuses increased the defense against herbivores and/or enhanced the dispersal of achenes. These morphological changes are associated with increases in diversity, suggesting that they might have played important roles in the elevated biodiversity of these groups.

CONCLUSIONS

We generated new transcriptome and genome datasets for 137 Asteraceae species and combined them with 106 other datasets (Zeng et al., 2014; Liu et al., 2015; Huang et al., 2016b) to provide a sample of 243 Asteraceae species, representing all 13 subfamilies and 41 of the 45 tribes, excluding only four small tribes with a total of nine species. These datasets were used to obtain >1,000 nuclear genes for phylogenetic analyses, molecular clock estimates, and analyses of diversification rate shifts, as well as >5,000 gene families for the phylogenomic detection of coincidental gene duplicates at multiple nodes in the Asteraceae phylogeny, providing strong evidence for 41 WGD events. The newly established nuclear Asteraceae phylogeny provides a well-supported resolution of most relationships among the sampled taxa, including the monophyly of eight of the 11 subfamilies containing more than one species and 30 of the 32 tribes with at least two species (Millerieae and Neurolaeneae are not shown to be monophyletic as currently circumscribed). In addition, this nuclear phylogeny is consistent with earlier plastid phylogenies for the relative placements of many subfamilies and tribes (see Panero and Crozier (2016) and references therein); however, several differences were found when comparing the plastid and nuclear phylogenies, some of which suggest possible hybrid origins of major lineages within the family. These include the phylogenetic positions of Cichorioideae, Pertyoideae, Stifftieae, Cichorieae, Hyalideae, Dicomeae, Anthemideae, Calenduleae, Gnaphalieae, all but two of the tribes of the Heliantheae alliance, and one genus each in Millerieae and Neurolaeneae. Three previously named subfamilies were found to be paraphyletic/polyphyletic, supporting the recognition of the tribe Dicomeae as the subfamily Dicomoideae, and the subfamily Vernonioideae for the clade containing the tribes Arctotideae, Liabeae, and Vernonieae. The two tribes of Wunderlichioideae are nested in different clades and may represent different subfamilies as well.

The well-resolved Asteraceae phylogeny proposed here provides the fundamental framework for further evolutionary analyses. Molecular clock estimates suggested that Asteraceae originated ~83 Mya in the late Cretaceous, that most early-divergent and small subfamilies diverged during the subsequent 10 My, and that further diversification, including the three largest subfamilies, occurred near the Cretaceous–Paleocene boundary (~66 Mya) (circles 2, 5–7 in Figure 3). Further diversification among most tribes was detected between the Eocene and the Paleocene (circle 4 in Figure 3). The results suggest that climate changes and the associated mass extinctions might have provided newly freed niches, which then were used by Asteraceae lineages that migrated to new locations and diversified, as supported by the proposed migration of the Asteraceae lineages (Mandel et al., 2019). Similar situations have also been suggested for Fabaceae, Solanaceae, and Poaceae (Vanneste et al., 2014b).

The Asteraceae topology at the tribal level and analyses of nuclear gene families from nearly all tribes allowed the detection of strong evidence for numerous WGDs using phylogenomic analyses. The detected WGDs are consistent with previous studies with smaller taxon samplings, including one shared by Asteraceae and its sister family Calyceraceae, one shared by the core Asteraceae (without Barnadesioideae and Famatinanthoideae), and one shared by the Heliantheae alliance (without/with Helenieae). In addition, a total of 32 candidate WGDs, some with minor support, were also proposed, including 19 in the largest subfamily, Asteroideae (Figure S35). Some candidate WGDs are associated with small subfamilies (WGD32 with Gymnarrhenoideae and WGD40 with Barnadesioideae), tribes (WGD21/WGD22 with Astereae, WGD23 with Gnaphalieae, and WGD37 with Wunderlichieae), or within a tribe (WGD29/WGD30 in Cichorioideae, and WGD33 in Cardueae). WGDs provide abundant genetic material for functional evolution, which likely contributed to morphological innovations, speciation, and adaptive radiation (Maere and Van de Peer, 2010; Arrigo and Barker, 2012). Such changes likely allowed organisms to take advantage of new ecological opportunities or cope with new environmental challenges, and might therefore have resulted in the expansion of biodiversity (Maere and Van de Peer, 2010; Schranz et al., 2012; Fawcett et al., 2013). Among the Asteraceae lineages, multiple pairs of sister clades (thus descendants of a common ancestor) exhibited great

differences in both species number and the number of detected WGD events shared by the corresponding clade and/or its subgroups, including: (i) Barnadesioideae (92 species and two WGDs) versus the remaining Asteraceae (~25,900 species (assuming the total Asteraceae species number is ~26,000) and 37 WGDs); (ii) Famatinanthoideae (one species and no WGD) versus the core Asteraceae (~25,900 species and 37 WGDs); (iii) the Mutisioideae–Stifftioideae clade (~690 species and five WGDs) versus the remaining core Asteraceae (~25,200 species and 31 WGDs); (iv) a grade of four successive sister branches (each with one to 85 species and zero or one WGD) of the clade Carduoideae–Asteroideae (~25,000 species and 29 WGDs); and (v) Corymbioideae (nine species and no WGD) versus Asteroideae (>17,000 species and 23 WGDs). The Asteraceae WGDs might therefore have contributed to the increases in biodiversity associated with the highly successful major clades of the family.

Furthermore, the reconstruction of ancestral morphological characters supports key morphological changes during the history of Asteraceae. One of these changes is from a woody to herbaceous habit after the separation of Pertyoideae from the common ancestor of the three largest subfamilies. This habit change postdated the WGD shared by the core Asteraceae, but predated the upshift in diversification rate associated with the node of both Asteroideae and Cichorioideae. In addition, the capitulum type transitioned from discoid to radiate-like, ligulate, and radiate in the ancestors of Mutisioideae, Cichorioideae I, Asteroideae, and Cichorioideae II, respectively, which likely contributed to enhanced pollinator attraction by the functionally "flower-like" heads and increased reproductive success. It is worth noting that the smaller clades (e.g., Barnadesioideae, Famatinanthoideae, Wunderlichioideae II, Gochnatioideae, Hecastocleidoideae, Pertyoideae, and Corymbioideae) in most pairs of sister clades with vastly different sizes mentioned in the previous paragraph have discoid capitula, in contrast to the larger sister clades with many taxa having heads with zygomorphic outer florets (Figure S39). In addition, among the early-divergent subfamilies, the Mutisioideae–Stifftioideae clade (~690 spp.) contains many taxa with radiate-like heads, and is larger than the others with discoid heads (species numbers from 1 to <100). The fact that the groups with "flower-like" heads are much larger than their sister clades suggests that the independent innovations in the capitulum likely contributed to their reproductive and evolutionary successes. Previous analyses have revealed that the MADS-box and *CYCLOIDEA2* (*CYC2*) floral regulatory genes duplicated since the origin of Asteraceae but before the divergence of Carduoideae I from Asteroideae and others, and that these genes play important roles in the development of the capitulum meristem and corolla in zygomorphic flowers (Chen et al., 2018; Elomaa et al., 2018). Furthermore, multiple innovations of the pappus, which can protect the achene and facilitate its dispersal, particularly those associated with the Heliantheae alliance, likely promoted the reproductive fitness and evolutionary success of the corresponding lineages. The association of these morphological changes with increases in diversity in these groups suggests that these morphological innovations are among the factors that could have contributed to the diversification of the family.

In summary, our analyses using a newly established Asteraceae nuclear phylogeny suggest environmental factors, including climate changes, and newly freed niches due to mass extinction, WGDs, and (subsequent) morphological innovations are some of the factors that likely contributed to the great biodiversity in Asteraceae, one of the two largest families of angiosperms. Some of the WGDs detected here likely provided new genetic materials for the evolution of novel functions, some of which might have supported morphological changes, such as the herbaceous habit for environmental adaptation (associated with the large clade containing all four of the largest subfamilies), the "flower-like" radiate head inflorescence with both peripheral ray flowers with large petals for pollinator attraction and central disc flowers for reproduction (associated with Asteroideae), and the pappus for seed dispersal. These morphological changes then facilitated the adaptation of the corresponding lineages during the periods following mass extinctions (at the Cretaceous–Paleocene and Eocene–Oligocene boundaries) and the promotion of the migration and expansion of Asteraceae from South America to other continents, with their descendants, especially those of the four largest subfamilies, eventually becoming distributed throughout most of the Earth's terrestrial and wetland ecosystems.

MATERIALS AND METHODS

Transcriptome and genome sequencing, selection of nuclear genes and phylogenetic analyses

RNAs were isolated from leaves and/or floral buds of 122 species representing major Asteraceae lineages (see Tables S1, S2). DNAs were extracted from dry samples for 16 other species. Transcriptome and genome shotgun sequencing were performed by using Illumina HiSeq2500 or HiSeq3000. The RNA/DNA sequencing raw reads were assembled with Trinity v2013-11-10 (Grabherr et al., 2011) and SOAPdenovo 2.04-r240 (Xie et al., 2014), respectively. The raw reads of newly generated samples in this study were uploaded into the National Center for Biotechnology Information databases (The BioProject accession number: PRJNA636629). Three sets of low-copy nuclear genes were obtained from the 244 Asteraceae datasets and five outgroup species, resulting in 1,087 OGs for phylogenetic analyses (Figure S2; Table S9). Coalescence and supermatrix phylogenetic reconstruction analyses were performed using ASTRAL 4.10.6 (Mirarab et al., 2014) and RaxML v7.0.4 (Stamatakis, 2006), respectively.

Divergence time estimations and analyses for net diversification rate shifts

A maximum likelihood tree using gene set 11 (Figure S2) with additional samplings of Asterales (Tables S1, S2) was reconstructed for molecular clock analyses. The ages of Asteraceae lineages were estimated using the penalized likelihood and Bayesian methods implemented respectively in

r8s v1.7.1 (Sanderson, 2003) and BEAST v2.4.3 (Bouckaert et al., 2014), using 14 or 15 fossils in five alternative calibration sets (see Supporting Information) mostly according to Smith et al. (2010), Magallón et al. (2015) and Panero and Crozier (2016). We used MEDUSA (Alfaro et al., 2009) implemented in the Geiger package (Harmon et al., 2008) of R (R Core Team, 2016) as well as the two algorithms (time-constant and time-variable algorithms) in BAMM v2.5 (Rabosky, 2014; Rabosky et al., 2014a, 2014b) (http://bamm-project.org/, last accessed November 6, 2016) to estimate the diversification rate shifts within Asteraceae.

Phylogenomic analyses for gene duplications as evidence for WGD

There were 6,059 OGs selected as a template from our previous study (Huang et al., 2016a) to search orthologous sequences of all species used in phylogenetic analyses, with the addition of five Asteraceae species (*Pertya phylicoides*, *Liabellum palmeri*, *Macledium spinosum*, *Palafoxia arida*, *Xanthopappus subacaulis*) which were sequenced more recently, to supplement the sampling of five corresponding tribes (Tables S1, S2). After selection of sequence quality, the remaining 5,282 OGs were used in subsequent reconstruction and mapping procedures. Gene trees were reconstructed using FastTree v2.1.4 (Price et al., 2009, 2010), and then the nodes of gene duplication in each gene tree were mapped and counted at the corresponding nodes in the species tree.

Reconstruction of ancestral states of morphological characters

Evolutionary histories of seven characters including habit, inflorescence, capitulum sexual differentiation, capitulum type, corollas in a capitulum, pappus and receptacular bract were estimated using Mesquite v3.10 (http://mesquiteproject.org) under a stochastic ML Markov k-state one-parameter model on a revised likelihood tree of combined 192 genes (set 11; Figure S2) with genus as unit. Details of the character matrix are provided in Table S6 (see Supporting Information for details).

ACKNOWLEDGEMENTS

We thank Beijing Botanical Garden, Bonn University Botanic Gardens, Guizhou Botanical Garden, Shanghai Chenshan Botanical Garden, South China Botanical Garden, Tel Aviv University Botanical Garden, UC Berkeley Botanical Garden, US Botanical Garden, Victoria Botanical Garden, and Zhihao Cheng, Zhixi Fu, Holly Forbes, Megan Hirst, Haihua Hu, Xiaojie Li, Fan Lu, Jinshuang Ma, Michal Monosov, Dunyan Tan, Huang-Lung Tsai, Weimin Ni, Li Song, Yaqiong Wang, Zehuan Wang, Ji Yang, Yushi Ye, Liping Zeng, Junwen Zhai, Guojin Zhang, Ning Zhang, and Shu Zhang for plant materials, Ji Qi for a script to map gene duplications, and Bao Nie, Wei Wang, and Guojin Zhang for technical assistance and discussion. This work was supported by funds from grants from the National Natural Science Foundation of China (Nos 31770242 and 31970224) and by funds from the Biology Department and the Huck Institutes of the Life Sciences at the Pennsylvania State University.

AUTHOR CONTRIBUTIONS

H.M. conceived of and designed the study. C.Z. selected the taxa and performed the phylogenetic analyses, and morphological character reconstruction. C.Z., M.L., H.M., Y.H., J.L.P., F.L., and T.G. contributed plant materials; C.Z. and Y.H. performed RNA and DNA isolation. M.L. performed preliminary phylogenetic analyses based on partial data. C.-H.H. designed and performed the dating and the diversification rate analyses and phylogenomics of whole genome duplication. C.Z., C.-H. H., and H.M. wrote the paper with contributions from all other authors. All authors read and approved the manuscript.

Edited by: Ya-Long Guo, Botany Institute of Botany, CAS, China

Received Aug. 21, 2020; **Accepted** Feb. 8, 2021; **Published** Feb. 9, 2021

OO: OnlineOpen

REFERENCES

Alfaro, M.E., Santini, F., Brock, C., Alamillo, H., Dornburg, A., Rabosky, D.L., Carnevale, G., and Harmon, L.J. (2009). Nine exceptional radiations plus high turnover explain species diversity in jawed vertebrates. Proc. Natl. Acad. Sci. USA **106:** 13410–13414.

Anderberg, A.A., Baldwin, B.G., Bayer, R.G., Breitwieser, J., Jeffrey, C., Dillon, M.O., Eldenäs, P., Funk, V., Garcia-Jacas, N., Hind, D.J.N., Karis, P.O., Lack, H.W., Nesom, G., Nordenstam, B., Oberprieler, C., Panero, J.L., Puttock, C., Robinson, H., Stuessy, T.F., Susanna, A., Urtubey, E., Vogt, R., Ward, J., and Watson, L.E. (2007). Compositae. In: J. Kadereit, C. Jeffrey, eds. *The Families and Genera of Vascular Plants, vol. 8. Flowering Plants, Eudicots, Asterales*, Springer. pp. 61–588.

Arrigo, N., and Barker, M.S. (2012). Rarely successful polyploids and their legacy in plant genomes. Curr. Opin. Plant Biol. **15:** 140–146.

Badouin, H., Gouzy, J., Grassa, C.J., Murat, F., Staton, S.E., Cottret, L., Lelandais-Brière, C., Owens, G.L., Carrère, S., Mayjonade, B., Legrand, L., Gill, N., Kane, N.C., Bowers, J.E., Hubner, S., Bellec, A., Bérard, A., Bergès, H., Blanchet, N., Boniface, M.-C., Brunel, D., Catrice, O., Chaidir, N., Claudel, C., Donnadieu, C., Faraut, T., Fievet, G., Helmstetter, N., King, M., Knapp, S.J., Lai, Z., Le Paslier, M.-C., Lippi, Y., Lorenzon, L., Mandel, J.R., Marage, G., Marchand, G., Marquand, E., Bret-Mestries, E., Morien, E., Nambeesan, S., Nguyen, T., Pegot-Espagnet, P., Pouilly, N., Raftis, F., Sallet, E., Schiex, T., Thomas, J., Vandecasteele, C., Varès, D., Vear, F., Vautrin, S., Crespi, M., Mangin, B., Burke, J.M., Salse, J., Muños, S., Vincourt, P., Rieseberg, L.H., and Langlade, N.B. (2017). The sunflower genome provides insights into oil metabolism, flowering and Asterid evolution. Nature **546:** 148–152.

Baldwin, B.G. (2009). Heliantheae alliance. In: V.A. Funk, A. Susana, T.F. Stuessy, R.J. Bayer, eds. *Systematics, Evolution and Biogeography of Compositae*, International Association for Plant Taxonomy. pp. 689–711.

Baldwin, B.G., Wessa, B.L., and Panero, J.L. (2002). Nuclear rDNA evidence for major lineages of helenioid Heliantheae (Compositae). Syst. Bot. **27:** 161–198.

Barker, M.S., Kane, N.C., Matvienko, M., Kozik, A., Michelmore, R.W., Knapp, S.J., and Rieseberg, L.H. (2008). Multiple paleopolyploidizations during the evolution of the Compositae reveal parallel patterns of duplicate gene retention after millions of years. Mol. Biol. Evol. **25:** 2445–2455.

Barker, M.S., Li, Z., Kidder, T.I., Reardon, C.R., Lai, Z., Oliveira, L.O., Scascitelli, M., and Rieseberg, L.H. (2016). Most Compositae (Asteraceae) are descendants of a paleohexaploid and all share a paleotetraploid ancestor with the Calyceraceae. Am. J. Bot. **103:** 1203–1211.

Barreda, V.D., Palazzesi, L., Tellería, M.C., Olivero, E.B., Raine, J.I., and Forest, F. (2015). Early evolution of the angiosperm clade Asteraceae in the Cretaceous of Antarctica. Proc. Natl. Acad. Sci. USA **112:** 10989–10994.

Barres, L., Sanmartín, I., Anderson, C.L., Susanna, A., Buerki, S., Galbany-Casals, M., and Vilatersana, R. (2013). Reconstructing the evolution and biogeographic history of tribe Cardueae (Compositae). Am. J. Bot. **100:** 867–882.

Beaulieu, J.M., Tank, D.C., and Donoghue, M.J. (2013). A southern hemisphere origin for campanulid angiosperms, with traces of the break-up of Gondwana. BMC Evol. Biol. **13:** 80.

Berry, S.T., Leon, A.J., Hanfrey, C.C., Challis, P., Burkholz, A., Barnes, S.R., Rufener, G.K., Lee, M., and Caligari, P.D. (1995). Molecular marker analysis of *Helianthus annuus* L. 2. Construction of an RFLP linkage map for cultivated sunflower. Theor. Appl. Genet. **91:** 195–199.

Bouckaert, R., Heled, J., Kühnert, D., Vaughan, T., Wu, C.H., Xie, D., Suchard, M.A., Rambaut, A., and Drummond, A.J. (2014). BEAST 2: A software platform for bayesian evolutionary analysis. PLoS Comp. Biol. **10:** e1003537.

Bremer, K. (1994). *Asteraceae: Cladistics and Classification*. Timber Press.

Bremer, K., Friis, E.M., and Bremer, B. (2004). Molecular phylogenetic dating of Asterid flowering plants shows early cretaceous diversification. Syst. Biol. **53:** 496–505.

Cannon, S.B., McKain, M.R., Harkess, A., Nelson, M.N., Dash, S., Deyholos, M.K., Peng, Y., Joyce, B., Stewart, C.N., Rolf, M., Kutchan, T., Tan, X., Chen, C., Zhang, Y., Carpenter, E., Wong, G.K.-S., Doyle, J.J., and Leebens-Mack, J. (2015). Multiple polyploidy events in the early radiation of nodulating and nonnodulating legumes. Mol. Biol. Evol. **32:** 193–210.

Celep, F., Atalay, Z., Dikmen, F., Dogan, M., and Classen-Bockhoff, R. (2014). Flies as pollinators of melittophilous *Salvia* species (Lamiaceae). Am. J. Bot. **101:** 2148–2159.

Chen, J., Shen, C., Guo, Y., and Rao, G. (2018). Patterning the Asteraceae capitulum: Duplications and differential expression of the flower symmetry *CYC2*-Like genes. Front. Plant Sci. **9:** 551.

Christenhusz, M.J.M., and Byng, J.W. (2016). The number of known plants species in the world and its annual increase. Phytotaxa **261:** 201–217.

Davies, T.J., Barraclough, T.G., Savolainen, V., and Chase, M.W. (2004). Environmental causes for plant biodiversity gradients. Philos. Trans. R. Soc. Lond. B. Biol. Sci. **359:** 1645–1656.

Elomaa, P., Zhao, Y., and Teng, Z. (2018). Flower heads in Asteraceae—Recruitment of conserved developmental regulators to control the flower-like inflorescence architecture. Hortic. Res. **5:** 36.

Fawcett, J.A., Van de Peer, Y., and Maere, S. (2013). Significance and biological consequences of polyploidization in land plant evolution. In: I.J. Leitch, ed. *Plant Genome Diversity*, Springer. pp. 277–294.

Fu, Z.X., Jiao, B.H., Nie, B., Zhang, G.J., and Gao, T.G. (2016). A comprehensive generic-level phylogeny of the sunflower family: Implications for the systematics of Chinese Asteraceae. J. Syst. Evol. **54:** 416–437.

Funk, V.A., Anderberg, A.A., Baldwin, B.G., Bayer, R.J., Bonifacino, J. M., Breitwieser, I., Brouillet, L., Carbajal, R., Chan, R., Coutinho, A. X.P., Crawford, D.J., Crisci, J.V., Dillon, M.O., Freire, S.E., Galbany-Casals, M., Garcia-Jacas, N., Gemeinholzer, B., Gruenstaeudl, M., Hansen, H.V., Himmelreich, S., Kaderei, J.W., Källersjö, M., Karaman-Castro, V., Karis, P.O., Katinas, L., Keeley, S.C., Kilian, N., Kimball, R.T., Lowrey, T.K., Lundberg, J., McKenzie, R.J., Tadesse, M.n, Mort, M.E., Nordenstam, B., Oberprieler, C., Santiago, O.rtiz, Pelser, P.B., Randle, C.P., Robinson, H., Roque, N., Sancho, G., Semple, J.C., Serrano, M., Stuessy, T.F., Susanna, A., Matthew, U. nwin, Urbatsch, L., Urtubey, E., Vallès, J., Vogt, R., Wagstaff, S., Ward, J., and Watson, L.E. (2009b). Compositae metatrees: The next generation. In: V.A. Funk, A. Susana, T.F. Stuessy, R.J. Bayer, eds. *Systematics, Evolution and Biogeography of Compositae*, International Association for Plant Taxonomy. pp. 747–777.

Funk, V.A., and Chan, R. (2009). Introduction to the Cichoroideae. In: V.A. Funk, A. Susanna, T.F. Stuessy, R.J. Bayer, eds. *Systematics, Evolution and Biogeography of Compositae*, International Association for Plant Taxonomy. pp. 335–342.

Funk, V.A., Chan, R., and Keeley, S.C. (2004). Insights into the evolution of the tribe Arctoteae (Compositae: Subfamily Cichorioideae S.S.) using *trnL-F*, *ndhF*, and ITS. Taxon **53:** 637–655.

Funk, V.A., Sancho, G., Roque, N., Kelloff, C.L., Ventosa-Rodríguez, I., Diazgranados, M., Bonifacino, J.M., and Chan, R. (2014). A phylogeny of the Gochnatieae: Understanding a critically placed tribe in the Compositae. Taxon **63:** 859–882.

Funk, V.A., Susanna, A., Stuessy, T.F., and Robinson, H. (2009a). Classification of *Compositae*. In: V.A. Funk, A. Susana, T.F. Stuessy, R. J. Bayer, eds. Systematics, Evolution and Biogeography of Compositae, International Association for Plant Taxonomy. pp. 171–189.

Gentzbittel, L., Vear, F., Zhang, Y.X., Berville, A., and Nicolas, P. (1995). Development of a consensus linkage RFLP map of cultivated sunflower (*Helianthus annuus* L.). Theor. Appl. Genet. **90:** 1079–1086.

Grabherr, M.G., Haas, B.J., Yassour, M., Levin, J.Z., Thompson, D.A., Amit, I., Adiconis, X., Fan, L., Raychowdhury, R., Zeng, Q., Chen, Z., Mauceli, E., Hacohen, N., Gnirke, A., Rhind, N., di Palma, F., Birren, B.W., Nusbaum, C., Lindblad-Toh, K., Friedman, N., and Regev, A. (2011). Full-length transcriptome assembly from RNA-Seq data without a reference genome. Nat. Biotechnol. **29:** 644–652.

Harmon, L.J. (2012). An inordinate fondness for eukaryotic diversity. PLoS Biol. **10:** e1001382.

Harmon, L.J., Weir, J.T., Brock, C.D., Glor, R.E., and Challenger, W. (2008). GEIGER: Investigating evolutionary radiations. Bioinformatics **24:** 129–131.

Huang, C.H., Sun, R.R., Hu, Y., Zeng, L.P., Zhang, N., Cai, L.M., Zhang, Q., Koch, M.A., Al-Shehbaz, I., Edger, P.P., Pires, J.C., Tan, D.Y., Zhong, Y., and Ma, H. (2016b). Resolution of Brassicaceae phylogeny using nuclear genes uncovers nested radiations and supports convergent morphological evolution. Mol. Biol. Evol. **33:** 394–412.

Huang, C.H., Zhang, C.F., Liu, M., Hu, Y., Gao, T.G., Qi, J., and Ma, H. (2016a). Multiple polyploidization events across Asteraceae with two nested events in the early history revealed by nuclear phylogenomics. Mol. Biol. Evol. **33:** 2820–2835.

Ivany, L.C., Patterson, W.P., and Lohmann, K.C. (2000). Cooler winters as a possible cause of mass extinctions at the Eocene/Oligocene boundary. Nature **407:** 887–890.

Jabaily, R.S., Shepherd, K.A., Gardner, A.G., Gustafsson, M.H.G., Howarth, D.G., and Motley, T.J. (2014). Historical biogeography of the predominantly Australian, plant family Goodeniaceae. J. Biogeogr **41:** 2057–2067.

Jablonski, D., and Chaloner, W.G. (1994). Extinctions in the fossil record: Discussion. Philos. Trans. R. Soc. Lond. B. Biol. Sci. **344:** 16–17.

Jablonski, D., Roy, K., and Valentine, J.W. (2006). Out of the tropics: Evolutionary dynamics of the latitudinal diversity gradient. Science **314:** 102–106.

Jansen, R.K., Michaels, H.J., and Palmer, J.D. (1991). Phylogeny and character evolution in the Asteraceae based on chloroplast DNA restriction site mapping. Syst. Bot. **16:** 98–115.

Jansson, R., and Davies, T.J. (2008). Global variation in diversification rates of flowering plants: Energy vs. climate change. Ecol. Lett. **11:** 173–183.

Jiao, Y., Wickett, N.J., Ayyampalayam, S., Chanderbali, A.S., Landherr, L., Ralph, P.E., Tomsho, L.P., Hu, Y., Liang, H., Soltis, P.S., Soltis, D. E., Clifton, S.W., Schlarbaum, S.E., Schuster, S.C., Ma, H., Leebens-Mack, J., and dePamphilis, C.W. (2011). Ancestral polyploidy in seed plants and angiosperms. Nature **473:** 97–100.

Karis, P.O., Funk, V.A., McKenzie, R.J., Barker, N.P., and Chan, R. (2009). Arctotideae. In: V.A. Funk, A. Susanna, T.F. Stuessy, R.J. Bayer, eds. *Systematics, Evolution and Biogeography of Compositae*, International Association for Plant Taxonomy, pp. 385–410.

Katinas, L., Pruski, J.F., Sancho, G., and Tellería, M.C. (2008). The subfamily Mutisioideae (Asteraceae). Bot. Rev. **74:** 469–716.

Leebens-Mack, J.H., Barker, M.S., Carpenter, E.J., Deyholos, M.K., Gitzendanner, M.A., Graham, S.W., Grosse, I., Li, Z., Melkonian, M., Mirarab, S., Porsch, M., Quint, M., Rensing, S.A., Soltis, D.E., Soltis, P.S., Stevenson, D.W., Ullrich, K.K., Wickett, N.J., DeGironimo, L., Edger, P. P., Jordon-Thaden, I.E., Joya, S., Liu, T., Melkonian, B., Miles, N.W., Pokorny, L., Quigley, C., Thomas, P., Villarreal, J.C., Augustin, M.M., Barrett, M.D., Baucom, R.S., Beerling, D.J., Benstein, R.M., Biffin, E., Brockington, S.F., Burge, D.O., Burris, J.N., Burris, K.P., Burtet-Sarramegna, V., Caicedo, A.L., Cannon, S.B., Çebi, Z., Chang, Y., Chater, C., Cheeseman, J.M., Chen, T., Clarke, N.D., Clayton, H., Covshoff, S., Crandall-Stotler, B.J., Cross, H., dePamphilis, C.W., Der, J.P., Determann, R., Dickson, R.C., Di Stilio, V.S., Ellis, S., Fast, E., Feja, N., Field, K.J., Filatov, D.A., Finnegan, P.M., Floyd, S.K., Fogliani, B., García, N., Gâteblé, G., Godden, G.T., Goh, F., Greiner, S., Harkess, A., Heaney, J.M., Helliwell, K.E., Heyduk, K., Hibberd, J.M., Hodel, R.G.J., Hollingsworth, P.M., Johnson, M.T.J., Jost, R., Joyce, B., Kapralov, M. V., Kazamia, E., Kellogg, E.A., Koch, M.A., Von Konrat, M., Könyves, K., Kutchan, T.M., Lam, V., Larsson, A., Leitch, A.R., Lentz, R., Li, F.W., Lowe, A.J., Ludwig, M., Manos, P.S., Mavrodiev, E., McCormick, M.K., McKain, M., McLellan, T., McNeal, J.R., Miller, R.E., Nelson, M.N., Peng, Y., Ralph, P., Real, D., Riggins, C.W., Ruhsam, M., Sage, R.F., Sakai, A.K., Scascitella, M., Schilling, E.E., Schlösser, E.-M., Sederoff, H., Servick, S., Sessa, E.B., Shaw, A.J., Shaw, S.W., Sigel, E.M., Skema, C., Smith, A.G., Smithson, A., Stewart, C.N., Stinchcombe, J.R., Szövényi, P., Tate, J.A., Tiebel, H., Trapnell, D., Villegente, M., Wang, C. N., Weller, S.G., Wenzel, M., Weststrand, S., Westwood, J.H., Whigham, D.F., Wu, S., Wulff, A.S., Yang, Y., Zhu, D., Zhuang, C., Zuidof, J., Chase, M.W., Pires, J.C., Rothfels, C.J., Yu, J., Chen, C., Chen, L., Cheng, S., Li, J., Li, R., Li, X., Lu, H., Ou, Y., Sun, X., Tan, X., Tang, J., Tian, Z., Wang, F., Wang, J., Wei, X., Xu, X., Yan, Z., Yang, F., Zhong, X., Zhou, F., Zhu, Y., Zhang, Y., Ayyampalayam, S., Barkman, T. J., Nguyen, N.-P., Matasci, N., Nelson, D.R., Sayyari, E., Wafula, E.K., Walls, R.L., Warnow, T., An, H., Arrigo, N., Baniaga, A.E., Galuska, S., Jorgensen, S.A., Kidder, T.I., Kong, H., Lu-Irving, P., Marx, H.E., Qi, X., Reardon, C.R., Sutherland, B.L., Tiley, G.P., Welles, S.R., Yu, R., Zhan, S., Gramzow, L., Theißen, G., Wong, G.K.-S., One Thousand Plant Transcriptomes Initiative. (2019). One thousand plant transcriptomes and the phylogenomics of green plants. Nature **574:** 679–685.

Leins, P., and Erbar, C. (2010). *Flower and Fruit: Morphology, Ontogeny, Phylogeny, Function and Ecology*. Schweizerbart Science Publishers.

Li, Z., Baniaga, A.E., Sessa, E.B., Scascitelli, M., Graham, S.W., Rieseberg, L.H., and Barker, M.S. (2015). Early genome duplications in conifers and other seed plants. Sci. Adv. **1:** e1501084.

Linnert, C., Robinson, S.A., Lees, J.A., Bown, P.R., Pérez-Rodríguez, I., Petrizzo, M.R., Falzoni, F., Littler, K., Arz, J.A., and Russell, E.E. (2014). Evidence for global cooling in the late Cretaceous. Nat. Commun. **5:** 4194.

Liu, M., Zhang, C.F., Huang, C.H., and Ma, H. (2015). Phylogenetic reconstruction of tribal relationships in Asteroideae (Asteraceae) with low-copy nuclear genes. Chin. Bull. Bot **50:** 549–564.

Loreau, M., Naeem, S., Inchausti, P., Bengtsson, J., Grime, J.P., Hector, A., Hooper, D.U., Huston, M.A., Raffaelli, D., Schmid, B., Tilman, D., and Wardle, D.A. (2001). Biodiversity and ecosystem functioning: Current knowledge and future challenges. Science **294:** 804–808.

Lughadha, E.N., Govaerts, R., Belyaeva, I., Black, N., Lindon, H., Allkin, R., Magill, R.E., and Nicolson, N. (2016). Counting counts: Revised estimates of numbers of accepted species of flowering plants, seed plants, vascular plants and land plants with a review of other recent estimates. Phytotaxa **272:** 82–88.

Maere, S., and Van de Peer, Y. (2010). Duplicate retention after small- and large-scale duplications. In: K. Dittmar, D. Liberles, eds. *Evolution after Gene Duplication*, Wiley, pp. 31–56.

Magallón, S., Gómez-Acevedo, S., Sánchez-Reyes, L.L., and Hernández-Hernández, T. (2015). A metacalibrated time-tree documents the early rise of flowering plant phylogenetic diversity. New Phytol. **207:** 437–453.

Mandel, J.R., Barker, M.S., Bayer, R.J., Dikow, R.B., Gao, T.G., Jones, K.E., Keeley, S., Kilian, N., Ma, H., Siniscalchi, C.M., Susanna, A., Thapa, R., Watson, L., and Funk, V.A. (2017). The Compositae tree of life in the age of phylogenomics. J. Syst. Evol. **55:** 405–410.

Mandel, J.R., Dikow, R.B., Funk, V.A., Masalia, R.R., Staton, S.E., Kozik, A., Michelmore, R.W., Rieseberg, L.H., and Burke, J.M. (2014). A target enrichment method for gathering phylogenetic information from hundreds of loci: An example from the Compositae. Appl. Plant Sci. 2: apps. **2:** 1300085.

Mandel, J.R., Dikow, R.B., Siniscalchi, C.M., Thapa, R., Watson, L. E., and Funk, V.A. (2019). A fully resolved backbone phylogeny reveals numerous dispersals and explosive diversifications throughout the history of Asteraceae. Proc. Natl. Acad. Sci. USA **116:** 14083–14088.

Mirarab, S., Reaz, R., Bayzid, M.S., Zimmermann, T., Swenson, M.S., and Warnow, T. (2014). ASTRAL: Genome-scale coalescent-based species tree estimation. Bioinformatics **30:** i541–i548.

Nordenstam, B. (2007). Tribe Senecioneae In: J. Kadereit, C. Jeffrey, eds. *The Families and Genera of Vascular Plants, vol. 8. Flowering Plants, Eudicots, Asterales*, Springer. pp. 208–241.

Nordenstam, B., Pelser, P.B., Kadereit, J.W., and Watson, L.E. (2009). Senecioneae. In: V.A. Funk, A. Susana, T.F. Stuessy, R.J. Bayer, eds. *Systematics, Evolution and Biogeography of the Compositae*, International Association for Plant Taxonomy. pp. 503–525.

Panero, J. (2005). New combinations and infrafamilial taxa in the Asteraceae. Phytologia **87:** 1–14.

Panero, J.L. (2007). Key to the tribes of the Heliantheae alliance, tribe Athroismeae, tribe Helenieae, tribe Coreopsideae, tribe Neurolaenae, tribe Tageteae, tribe Chaenactideae, tribe Bahieae, tribe Polymnieae, tribe Heliantheae, tribe Millerieae, tribe Perityleae. In: J. Kadereit, C. Jeffrey, eds. *The Families and Genera of Vascular Plants, vol. 8. Flowering Plants, Eudicots, Asterales*, Springer. pp. 391–477, 507–510.

Panero, J.L. (2016). Phylogenetic uncertainty and fossil calibration of Asteraceae chronograms. Proc. Natl. Acad. Sci. USA **113:** E411.

Panero, J.L., and Crozier, B.S. (2016). Macroevolutionary dynamics in the early diversification of Asteraceae. Mol. Phylogen. Evol. **99:** 116–132.

Panero, J.L., Francisco-Ortega, J., Jansen, R.K., and Santos-Guerra, A. (1999). Molecular evidence for multiple origins of woodiness and a new world biogeographic connection of the Macaronesian Island endemic *Pericallis* (Asteraceae: Senecioneae). Proc. Natl. Acad. Sci. USA **96:** 13886–13891.

Panero, J.L., Freire, S.E., Ariza Espinar, L., Crozier, B.S., Barboza, G.E., and Cantero, J.J. (2014). Resolution of deep nodes yields an improved backbone phylogeny and a new basal lineage to study early evolution of Asteraceae. Mol. Phylogen. Evol. **80:** 43–53.

Panero, J.L., and Funk, V.A. (2002). Toward a phylogentic subfamilial classification for the *Compositae* (*Asteraceae*). Proc. Biol. Soc. Wash. **115:** 760–773.

Panero, J.L., and Funk, V.A. (2008). The value of sampling anomalous taxa in phylogenetic studies: Major clades of the Asteraceae revealed. Mol. Phylogen. Evol. **47:** 757–782.

Park, D.S., and Potter, D. (2015). Why close relatives make bad neighbours: Phylogenetic conservatism in niche preferences and dispersal disproves Darwin's naturalization hypothesis in the thistle tribe. Mol. Ecol. **12:** 3181–3193.

Pelser, P.B., Kennedy, A.H., Tepe, E.J., Shidler, J.B., Nordenstam, B., Kadereit, J.W., and Watson, L.E. (2010). Patterns and causes of incongruence between plastid and nuclear Senecioneae (Asteraceae) phylogenies. Am. J. Bot. **97:** 856–873.

Price, M.N., Dehal, P.S., and Arkin, A.P. (2009). FastTree: Computing large minimum evolution trees with profiles instead of a distance matrix. Mol. Biol. Evol. **26:** 1641–1650.

Price, M.N., Dehal, P.S., and Arkin, A.P. (2010). FastTree 2 – Approximately maximum-likelihood trees for large alignments. PLoS One **5:** e9490.

R Core Team. (2016). *R: A language and environment for statistical computing*. R Foundation for Statistical Computing. https://www.R-project.org

Rabosky, D.L. (2014). Automatic detection of key innovations, rate shifts, and diversity-dependence on phylogenetic trees. PLoS One **9:** e89543.

Rabosky, D.L., Donnellan, S.C., Grundler, M., and Lovette, I.J. (2014a). Analysis and visualization of complex macroevolutionary dynamics: An example from Australian scincid lizards. Syst. Biol. **63:** 610–627.

Rabosky, D.L., Grundler, M., Anderson, C., Title, P., Shi, J.J., Brown, J. W., Huang, H., and Larson, J.G. (2014b). BAMMtools: An R package for the analysis of evolutionary dynamics on phylogenetic trees. Methods Ecol. Evol. **5:** 701–707.

Rabosky, D.L., Slater, G.J., and Alfaro, M.E. (2012). Clade age and species richness are decoupled across the eukaryotic tree of life. PLoS Biol. **10:** e1001381.

Ren, R., Wang, H., Guo, C.C., Zhang, N., Zeng, L.P., Chen, Y., Ma, H., and Qi, J. (2018). Widespread whole genome duplications contribute to genome complexity and species diversity in Angiosperms. Mol. Plant **11:** 414–428.

Reyes-Chin-Wo, S., Wang, Z., Yang, X., Kozik, A., Arikit, S., Song, C., Xia, L., Froenicke, L., Lavelle, D.O., Truco, M.-J., Xia, R., Zhu, S., Xu, C., Xu, H., Xu, X., Cox, K., Korf, I., Meyers, B.C., and Michelmore, R.W. (2017). Genome assembly with in vitro proximity ligation data and whole-genome triplication in lettuce. Nat. Commun. **8:** 14953.

Robinson, H. (1978). Studies in the Heliantheae (Asteraceae). XII. Reestablishment of the genus *Smallanthus*. Phytologia **39:** 47–53.

Robinson, H. (1981). A revision of the tribal and subtribal limits of the Heliantheae (Asteraceae). Smithson. Contrib. Bot. **51:** 1–102.

Robinson, H. (2004). New supertribes Helianthodae and Senecionodae, for the subfamily Asteroideae (Asteraceae). Phytologia **86:** 116–120.

Robinson, H. (2009). Moquinieae. In: V.A. Funk, A. Susana, T.F. Stuessy, R.J. Bayer, eds. *Systematics, Evolution and Biogeography of Compositae*, International Association for Plant Taxonomy. pp. 477–481.

Robinson, H., and Funk, V.A. (2009). Eremothamneae. In: V.A. Funk, A. Susana, T.F. Stuessy, R.J. Bayer, eds. *Systematics, Evolution and Biogeography of Compositae*, International Association for Plant Taxonomy. pp. 411–416.

Sanderson, M.J. (2003). r8s: Inferring absolute rates of molecular evolution and divergence times in the absence of a molecular clock. Bioinformatics **19:** 301–302.

Schranz, E.M., Mohammadin, S., and Edger, P.P. (2012). Ancient whole genome duplications, novelty and diversification: The WGD radiation lag-time model. Curr. Opin. Plant Biol. **15:** 147–153.

Semple, J.C., and Watanabe, K. (2009). A review of chromosome numbers in Asteraceae with hypotheses on chromosomal base number evolution. In: V.A. Funk, A. Susanna, T.F. Stuessy, R.J. Bayer, eds. *Systematics, Evolution and Biogeography of Compositae*, International Association for Plant Taxonomy. pp. 61–72.

Shi, J.J., and Rabosky, D.L. (2015). Speciation dynamics during the global radiation of extant bats. Evolution **69:** 1528–1545.

Smith, E. (1975). The chromosome numbers of North American *Coreopsis* with phyletic interpretations. Bot. Gaz. **136:** 78–86.

Smith, S.A., Beaulieu, J.M., and Donoghue, M.J. (2010). An uncorrelated relaxed-clock analysis suggests an earlier origin for flowering plants. Proc. Natl. Acad. Sci. USA **107:** 5897–5902.

Soltis, P.S., Marchant, D.B., Van de Peer, Y., and Soltis, D.E. (2015). Polyploidy and genome evolution in plants. Curr. Opin. Genet. Dev. **35:** 119–125.

Stamatakis, A. (2006). RAxML-VI-HPC: Maximum likelihood-based phylogenetic analyses with thousands of taxa and mixed models. Bioinformatics **22:** 2688–2690.

Stuessy, T.F., and Garver, D. (1996). The defensive role of pappus in heads of Compositae. In P.D.S. Caligari and D.J.N. Hind (Eds.), *Compositae: Biology and Utilization. Proceedings of the International Compositae Conference, Kew, 1994. Vol. 2*. Royal Botanical Gardens. pp. 81–91.

Stuessy, T.F., and Spooner, D.M. (1988). The adaptive and phylogenetic significance of receptacular bracts in the Compositae. Taxon **37:** 114–126.

Stuessy, T.F., Spooner, D.M., and Evans, K.A. (1986). Adaptive significance of ray corollas in *Helianthus grosseserratus* (Compositae). Am. Midl. Nat. **115:** 191–197.

Stuessy, T.F., Urtubey, E., and Gruenstaeudl, M. (2009). Barnadesieae (Barnadesioideae). In: V.A. Funk, A. Susanna, T.F. Stuessy, R.J. Bayer, eds. *Systematics, Evolution and Biogeography of Compositae*, International Association for Plant Taxonomy. pp. 215–228.

Tank, D.C., Eastman, J.M., Pennell, M.W., Soltis, P.S., Soltis, D.E., Hinchliff, C.E., Brown, J.W., Sessa, E.B., and Harmon, L.J. (2015). Nested radiations and the pulse of angiosperm diversification: Increased diversification rates often follow whole genome duplications. New Phytol. **207:** 454–467.

Vanneste, K., Baele, G., Maere, S., and Van de Peer, Y. (2014b). Analysis of 41 plant genomes supports a wave of successful genome duplications in association with the Cretaceous-Paleogene boundary. Genome Res. **24:** 1334–1347.

Vanneste, K., Maere, S., and Van de Peer, Y. (2014a). Tangled up in two: A burst of genome duplications at the end of the Cretaceous and the consequences for plant evolution. Philos. Trans. R. Soc. London. Ser. B. **369:** 5042–5050.

Wang, J.M. (2009). *Studies on Cytology and Leaf Epidermal Micromorphology of the Genus* Ainslaea (*Asteraceae*) (Master's thesis). Qufu Normal University, Qufu.

Willis, K.J. (2017). *State of the World's Plants 2017: Report*. Royal Botanic Gardens, London.

Xiang, Y.Z., Huang, C.H., Hu, Y., Wen, J., Li, S.S., Yi, T.S., Chen, H.Y., Xiang, J., and Ma, H. (2016). Evolution of Rosaceae fruit types based on nuclear phylogeny in the context of geological times and genome duplication. Mol. Biol. Evol. **34:** 262–281.

Xie, Y., Wu, G., Tang, J., Luo, R., Patterson, J., Liu, S., Huang, W., He, G., Gu, S., Li, S., Zhou, X., Lam, T.W., Li, Y., Xu, X., Wong, G.K., and Wang, J. (2014). SOAPdenovo-Trans: De novo transcriptome assembly with short RNA-Seq reads. Bioinformatics **30:** 1660–1666.

Yahara, T., Kawahara, T., Crawford, D.J., Ito, M., and Watanabe, K. (1989). Extensive gene duplications in diploid *Eupatorium* (Asteraceae). Am. J. Bot. **76:** 1247–1253.

Yang, Y., Moore, M.J., Brockington, S.F., Soltis, D.E., Wong, G.K.-S., Carpenter, E.J., Zhang, Y., Chen, L., Yan, Z.X., Xie, Y.L., Sage, R.F., Covshoff, S., Hibberd, J.M., Nelson, M.N., and Smith, S.A. (2015). Dissecting molecular evolution in the highly diverse plant clade Caryophyllales using transcriptome sequencing. Mol. Biol. Evol. **32:** 2001–2014.

Zanne, A.E., Tank, D.C., Cornwell, W.K., Eastman, J.M., Smith, S.A., FitzJohn, R.G., McGlinn, D.J., O'Meara, B.C., Moles, A.T., Reich, P. B., Royer, D.L., Soltis, D.E., Stevens, P.F., Westoby, M., Wright, I.J., Aarssen, L., Bertin, R.I., Calaminus, A., Govaerts, R., Hemmings, F., Leishman, M.R., Oleksyn, J., Soltis, P.S., Swenson, N.G., Warman,

L., and Beaulieu, J.M. (2014). Three keys to the radiation of angiosperms into freezing environments. Nature **506:** 89–92.

Zeng, L.P., Zhang, Q., Sun, R.R., Kong, H.Z., Zhang, N., and Ma, H. (2014). Resolution of deep angiosperm phylogeny using conserved nuclear genes and estimates of early divergence times. Nat. Commun. **5:** 4956.

Zeng, L.P., Zhang, N., Zhang, Q., Endress, P.K., Huang, J., and Ma, H. (2017). Resolution of deep eudicot phylogeny and their temporal diversification using nuclear genes from transcriptomic and genomic datasets. New Phytol. **214:** 1338–1354.

Zhang, C.F. (2013). *A Systematic Study of the Genus* Pertya *Sch.Bip. (Asteraceae)* (Doctoral Thesis). University of Chinese Academy of Sciences, Beijing.

Zhang, C.F., Zhang, T.K., Luebert, F., Xiang, Y.Z., Huang, C.H., Hu, Y., Rees, M., Frohlich, M.W., Qi, J., Weigend, M., and Ma, H. (2020). Asterid phylogenomics/phylotranscriptomics uncover morphological evolutionary histories and support phylogenetic placement for numerous whole genome duplications. Mol. Biol. Evol. **37:** 3188–3210.

SUPPORTING INFORMATION

Additional Supporting Information may be found online in the supporting information tab for this article: http://onlinelibrary.wiley.com/doi/10.1111/jipb.13078/suppinfo

Figure S1. Comparison of Asteraceae phylogenies at tribal level

The taxon names in maroon are present in Mandel et al. (2019) not in this study, while those in green are present in this study not in Mandel et al. Mandel et al. (2019) and those in blue are not included in Mandel et al. (2019) nor in this study. Subfamily abbreviations: Aster, Asteroideae; Ci-I, Cichorioideae I; Ci-II, Cichorioideae II; Ca-I, Carduoideae I; Ca-II, Carduoideae II; Muti, Mutisioideae. Subclades in tribes: Arctotideae I, Arctotidinae; Arctotideae II, Gorteriinae; Arctotideae III, *Heterolepis*; Neurolaeneae I, Neurolaeneae excluding *Enydra*; Neurolaeneae II, *Enydra*; Millerieae I, Millerieae excluding *Guardiola*; Millerieae II, *Guardiola*. Four among the subfamily-level clades with multiple tribes are highlighted with different colored backgrounds. Support values (%) less than 80 are given. Dashed lines indicate inconsistent relationships among different analyses in this study. **Jaumea* sampled in this study but not in Mandel et al. (2019) is excluded for comparison. **Including *Calendula arvensis*, a species of tribe Calenduleae, in Mandel et al. (2019).

Figure S2. A flow chart for gene selection approaches (**A**) and guide species trees (**B, C**) for gene selection

(**A**) Each blue rectangle represent a gene set starting with the 4,180 OGs (orthogroups, indicated with an asterisk) as described in the Supplemental Information. Gene sets 1-11 are indicated by a number within one of the other blue rectangles. Selection criteria are briefly indicated, with more information provided in the Supplemental Information. Gene set 3 with 175 genes from Huang et al. (2016b is indicated with two asterisks (SCOS, single-copy orthologous set). OGs, orthogroups. (**B**) A guide tree for selection gene set 2. Names of tribes are indicated to the right of the species names. Only the monophyly of Asteraceae and the included tribes are used; these relationships are supported by both the previous molecular phylogenies and the nuclear phylogeny here. (**C**) A guide tree used in a late step shown in part A, with monophyly for Asteraceae and the largest subfamily Asteroideae, both strongly supported by previous results and the analyses here. Ten genes in gene set 9 that were not consistent with this tree were removed, resulting in gene set 11, which was used for both coalescent and ML analyses.

Figure S3. A phylogenetic tree of Asteraceae using coalescent analysis with gene set 1 of 847 genes

Subfamilies are indicated on the right and highlighted with different background colors; tribes are marked with a vertical thick line, with names shown to the right of species names. Non-monophyletic subfamilies and tribes are shown with numbers I and II after the previous subfamily and tribe names. Bootstrap values of 100 are not shown, with those less than 100 shown next to the line for the lineage.

Figure S4. A phylogenetic tree of Asteraceae using coalescent analysis with gene set 2 of 177 genes

Figure S5. A phylogeny of Asteraceae using coalescent analysis with gene set 3 of 175 genes

Figure S6. A phylogeny of Asteraceae using coalescent analysis with gene set 4 of 1 087 genes

Figure S7. A phylogeny of Asteraceae using coalescent analysis with gene set 5 of 649 genes

Figure S8. A phylogeny of Asteraceae using coalescent analysis with gene set 6 of 438 genes

Figure S9. A phylogeny of Asteraceae using coalescent analysis with gene set 7 of 384 genes

Figure S10. A phylogeny of Asteraceae using coalescent analysis with gene set 8 of 265 genes

Figure S11. A phylogeny of Asteraceae using coalescent analysis with gene set 9 of 202 genes

Figure S12. A phylogeny of Asteraceae using coalescent analysis with gene set 11 of 192 genes

Figure S13. A phylogeny of Asteraceae using coalescent 192 nuclear analysis with genes with 800–1,000 bp (set 10)

Figure S14. A maximum likelihood phylogeny of Asteraceae using 192 genes (set 11)

Figure S15. A summary of support values from multiple phylogenies

The bootstrap values are shown next to the corresponding branches, in the same order (and matching colors) as that shown in the small diagram at the upper left part: the numbers indicate the number of genes used in an analysis, ML, Maximum Likelihood; Col, coalescent. The five results above the line (except that from 202 genes) are summarized in Figures 1 and 2. See Figure S2 legend for more information on taxa.

Figure S16. Divergence times estimated using r8s (calibration set 1)

Values are ages of each node. Calibrations were depicted with red circles. Information of all the constraints is provided in Table S3.

Figure S17. Divergence times estimated using BEAST (calibration set 1)

Values are mean ages of each node and the blue strips illustrate 95% highest posterior distribution (HPD). Fossil and secondary calibrations were the same as those in r8s analyses of the same calibration set. Information of all the constraints is provided in Table S3.

Figure S18. Divergence times estimated using r8s (calibration set 2)

Figure S19. Divergence times estimated using BEAST (calibration set 2)

Figure S20. Divergence times estimated using r8s (calibration set 3)

Figure S21. Divergence times estimated using BEAST (calibration set 3)

Figure S22. Divergence times estimated using r8s (calibration set 4)

Figure S23. Divergence times estimated using BEAST (calibration set 4)

Figure S24. Divergence times estimated using r8s (calibration set 5)

Figure S25. Divergence times estimated using BEAST (calibration set 5)

Figure S26. Comparison of ages with calibration sets 1 and 2 using r8s

This figure presents the nodal ages ordered by their ages from set 1 (red). The two nodes with large variations in ages between sets 1 and 2 are MRCA *Dasyphyllum-Arnaldoa* and crown Barnadesioideae (noted near the points).

Figure S27. Comparison of ages with calibration sets 1 and 2 using BEAST

This figure presents the nodal ages ordered by their ages from calibration set 1 (red). Colored lines show their 95% HPD. The two nodes with large variations in ages between calibration sets 1 and 2 are MRCA *Dasyphyllum-Arnaldoa* and crown Barnadesioideae (noted near the points).

Figure S28. Net diversification rate shift from analysis by MEDUSA under mixed model

This figure is the result of MEDUSA analysis using mixed model in the estimation. Colors indicate the diversification rates for branches; branches descending from a shift basically have the same rate (the same branch color) unless there is other shift(s). The type of a shift (up or down) was determined by comparing rates of branches directly upstream or downstream to the shift. Red and blue circles are the concluded types of shift nodes with net diversification rate accelerations and slowdowns, respectively. The order of the numbers on the circles is determined by the stepwise AIC procedure. The improved AIC scores (ΔAIC) and net diversification rates (Rate) are presented on the table in upper left of the figure. Green and blue dashed lines indicate the geological times of the K-P and E-O boundary, respectively. There is no extinction rate here because the shifts were fitted to the pure birth (Yule) model by MEDUSA.

Figure S29. Net diversification rate shift from analysis by MEDUSA under birth-death model

This analysis is nearly the same as that shown in Figure S28 except the

model was set to birth-death model. ε is the relative extinction rate as extinction rate (μ) / speciation rate (λ).

Figure S30. Shift configuration of net diversification rates with the highest maximum a posteriori (MAP) probability ("the best shift configuration") as a result of BAMM analyses

The highest maximum a posteriori (MAP) probability ("the best shift configuration") was obtained from BAMM analyses using time-constant and -variable algorithms, as shown in (**A**) and (**B**), respectively. Net diversification rates along branches are depicted with different colors with the rate dynamics. Red circles are core-shifts in the "best" shift configurations suggested by BAMM, which are the same as the first configuration in credible configuration sets (Figure S32D).

Figure S31. Rate-through-time (RTT) plots of net diversification rates estimated by BAMM

Results from time-constant and -variable algorithms are provided in (**A**) and (**B**), respectively. Positions of the numbered nodes are shown in Figure S34. Plots with purple are from data of complete tree, whereas those with red and cyan are clade rates from data of clades of the indicated nodes and the background rates excluding the corresponding clades, respectively. The unit of time (x-axis) is million years, and that of diversification rates (y-axis) is species per million years.

Figure S32. In-depth investigation on the shift positions from BAMM

(**A**) The prior (blue) and posterior (red) probabilities for each shift model by time-constant and time-variable algorithms, respectively. (**B**) The pairwise Bayes factors for all sampled shift models relative to the model with three shifts. (**C**) Frequencies of shift nodes sampled in five- to eight-shift models by time-constant algorithm in BAMM. Nodes that can be classified into five groups by their phylogenetic positions are denoted with names at topright. Values on each data point are the numbers the node to be identified as having rate shift, and those shown after the clade name are the sum for nodes belonging to the same group. Identities of nodes are shown in Figure S34. (D) The first nine credible shift sets (CSS, as defined in BAMM) for core-shifts of net diversification rates resulted from estimations by time-constant algorithm using BAMM. Frequencies of the samples in posterior assigned to each shift configuration are shown as the f values above each plot. Circles denote the place and probabilities (as relative size) of each rate shift at the node.

Figure S33. Cohorts of net diversification rates by BAMM

Colors from red to blue illustrate whether any two terminals in the tree share were in the same rate regime (red) or different rate regimes (blue). The major difference in the two algorithms (**A** and **B**) is in the color of blocks comparing Helianthodae (including the two possible rate shifts at the Heliantheae alliance and Eupatorieae) and some other clades in the clade of Asteroideae-Dicomeae (with dark blue branches), which are light blue in time-constant algorithm but are orange red in time-variable algorithm. This indicates that, in the clade of Asteroideae-Dicomeae, the rates of green branches (Helianthodae) are in different rate regimes from the dark blue branches in time-constant algorithm, whereas in time-variable algorithm the difference is eliminated.

Figure S34. Identification of modes in BAMM analyses

Figure S35. A summary of detected (candidate) whole genome duplication event

The detected WGDs were marked at the node. The red one are WGDs with relatively strong evidence, whereas the orange ones are WGDs with moderate supports (candidate WGDs, see the methods for details). The numbers represent the count of the gene duplication numbers, gene families and its ratio. The phylogenetic positions of the five species included in WGD analyses but not in phylogenetic analyses (Table S1) were supported by the ML tree based on the gene set 11 with 192 genes (Figure S2).

Figure S36. Ancestral character reconstruction of habit in Asteraceae

Figure S37. Ancestral character reconstruction of inflorescence in Asteraceae

Figure S38. Ancestral character reconstruction of capitulum sexual differentiation in Asteraceae

Figure S39. Ancestral character reconstruction of capitulum type in Asteraceae

Figure S40. Ancestral character reconstruction of corollas in a capitulum in Asteraceae

Figure S41. Ancestral character reconstruction of pappus in Asteraceae

Figure S42. Ancestral character reconstruction of receptacular bract in Asteraceae

Table S1. Taxa included in this study

Table S2. Statistics of newly sequenced transcriptomes and genomes

Table S3. Calibrations implemented in this study for divergence time

Table S4. Ages of clades of interest from BEAST and r8s analyses

Table S5. Sampling fractions for BAMM analyses

Table S6. Matrix of seven morphological characters

Table S7. List of 36 species used for selecting putative orthologous genes for Asteraceae from 4 180 ORGs

Table S8. Species coverage and average copies of the 4 180 putative orthologous genes in the 36 species

Table S9. Statistics of genes used in this study